THE ANTENNA LABORATORY

RESEARCH ACTIVITIES in ---

Automatic Controls — *Antennas* — *Echo Area Studies*
Microwave Circuits — *Astronautics* — *E M Field Theory*
Terrain Investigations — *Radomes* — *Systems Analysis*
Wave Propagation — *Submillimeter Applications*

An Investigation of a Method of Determining Antenna Parameters by Scattering Cross Section Measurements

S. J. Skarote

Grant Number NsG-448

1691-11

15 May 1965

Prepared for:
National Aeronautics and Space Administration
Office of Grants and Research Contracts
Washington, D. C. 20546

Department of ELECTRICAL ENGINEERING

THE OHIO STATE UNIVERSITY
RESEARCH FOUNDATION
Columbus, Ohio

NOTICES

When Government drawings, specifications, or other data are used for any purpose other than in connection with a definitely related Government procurement operation, the United States Government thereby incurs no responsibility nor any obligation whatsoever, and the fact that the Government may have formulated, furnished, or in any way supplied the said drawings, specifications, or other data, is not to be regarded by implication or otherwise as in any manner licensing the holder or any other person or corporation, or conveying any rights or permission to manufacture, use, or sell any patented invention that may in any way be related thereto.

The Government has the right to reproduce, use, and distribute this report for governmental purposes in accordance with the contract under which the report was produced. To protect the proprietary interests of the contractor and to avoid jeopardy of its obligations to the Government, the report may not be released for non-governmental use such as might constitute general publication without the express prior consent of The Ohio State University Research Foundation.

Qualified requesters may obtain copies of this report from the Defense Documentation Center, Cameron Station, Alexandria, Virginia. Department of Defense contractors must be established for DDC services, or have their "need-to-know" certified by the cognizant military agency of their project or contract.

REPORT 1691-11

REPORT

by

THE OHIO STATE UNIVERSITY RESEARCH FOUNDATION
COLUMBUS, OHIO 43212

Sponsor	National Aeronautics and Space Administration Office of Grants and Research Contracts Washington, D. C. 20546
Grant Number	NsG-448
Investigation of	Spacecraft Antenna Problems
Subject of Report	An Investigation of a Method of Determining Antenna Parameters by Scattering Cross Section Measurements
Submitted by	S. J. Skarote Antenna Laboratory Department of Electrical Engineering
Date	15 May 1965

The material contained in this report is also used as a thesis submitted to the Department of Electrical Engineering, The Ohio State University as partial fulfillment for the degree Master of Science.

ABSTRACT

27474

An error analysis of a scattering method for determining input impedance, gain, and cross section of an antenna is presented. Results obtained using the scattering method in conjunction with a calibrated, programmed load with signaling provisions are compared to those obtained using standard antenna measurement techniques.

An alternate method for determining antenna parameters by the scattering method which employs a simpler non-programmed load is described.

Author

CONTENTS

ACKNOWLEDGEMENT

The helpful discussions with R. J. Garbacz, D. L. Moffatt, and Dr. E. M. Kennaugh are sincerely appreciated; the guidance and interesting and helpful discussions of my adviser, Dr. C. H. Walter, are especially acknowledged.

CHAPTER I
INTRODUCTION

The purpose of this work is to describe a scattering method of measuring gain, impedance, and scattering cross section of an antenna and to compare this method with conventional methods of measuring gain and impedance. A review of conventional methods is given in Appendix A.

Gain and impedance measurements of several antennas employing the different methods are compared and a procedure for estimating error in the scattering method is presented. The original formulation of the scattering method[1] utilized a programmed load. An alternate approach making use of a simpler non-programmed load is presented.

In a scattering system (see Appendix A for details on a typical scattering system) an electromagnetic wave incident on a target is reradiated back to the receiving antenna, the magnitude and phase of the reradiation depending upon the material, shape, position, and orientation of the target and upon the frequency and polarization of the incident wave. The power, W, reflected back toward the receiver is related to the incident power density at the scatterer by[2]

$$W \propto \sigma S, \tag{1}$$

where S is the power density at the scatterer (assumed to be uniformly illuminated) and σ is defined as the scattering cross section or echo area of the scatterer.

If the scattering object is an antenna, the reradiation consists of a fixed component due to antenna and support structures and a load-dependent component due to the antenna mode. An analytical expression representing the total cross section in terms of the fixed and load-dependent components is of the form

$$\sigma = \kappa \left| \Gamma_1 \right|^2, \tag{2}$$

where κ is a calibrated constant of the radar system and Γ_1 is intepreted as a reflection coefficient given by

$$\Gamma_1 = B(C + \Gamma_m), \tag{3}$$

where B and C are constants and Γ_m is a load-dependent, modified, reflection coefficient (see Appendix B for details).

If the maximum, minimum, and average scattering cross sections and the corresponding purely reactive loads at the scattering antenna terminals are known, the input impedance of the scattering antenna may be found, its gain calculated, and its echo area for any load predicted. The maximum echo area, σ_{max}, is the maximum possible total cross section of the scattering antenna for a purely reactive load. Similarly, the minimum echo area, σ_{min}, is the

minimum cross section for a purely reactive load. The average scattering cross section is defined by

$$\sigma_{avg} = \frac{\sigma_{max} + \sigma_{min}}{2} \quad . \tag{4}$$

The necessary information which leads to determining the antenna gain and impedance parameters via simple graphical constructions can be obtained from an experimentally measured echo-area-versus-load curve (see Appendix B).

The conventional method of measuring gain requires the use of an antenna range and a standard gain antenna as reference. The details of this method are reviewed in Appendix A.

The common method of measuring impedance is by a slotted line which is used to measure the standing wave in a transmission line connected to the unknown impedance. The standing wave is related to the characteristic impedance of the transmission line and the terminating impedance in question. The details of the method are reviewed in Appendix A.

For a broader understanding of the scattering method of determining antenna parameters, several advantages and disadvantages of the method are presented. The scattering method is advantageous in situations where cables, measuring equipment, and operator may affect the results, e. g., where the antenna is located on a small body (for example, a radial stub on a sphere has been measured by

this method as described in Reference 3); where disturbances may be significant (in cases of low gain or omnidirectional antennas); and where coupling effects are under investigation. Parameters of coupled antennas may be determined by the scattering technique in which the antennas are excited with a common plane wave rather than having each antenna excited separately. Certain environments, such as high temperature regions, may be intolerable to cables and measuring equipment, but suitable to the programmed load used in the scattering method. Antennas located in remote places, such as aerospace vehicles, may be investigated by the scattering technique. Finally, the magnitude and phase of the load-independent or fixed scattering component of the antenna and supporting structure can be found from amplitude measurements alone.

The disadvantages of the scattering method are (1) the need of a programmed load with signaling provisions to correlate the echo area and the associated load, and (2) a relatively complex measuring system.

An alternate approach for determining antenna parameters by the scattering method employs a load without signaling provisions. An analysis of this method is presented in Section IV. In this method the load has essentially no signaling error, is physically smaller than the programmed load, and does not require a fast recorder to follow the periodic disturbances required to correlate the echo area with the associated load in the programmed-load method. Also, the

periodic disturbances of the programmed-load method may be difficult to observe when the load-dependent component is small compared to the fixed scattering component. The advantages of the simpler load are gained at the expense of a somewhat more complicated procedure for calculating the antenna parameters.

CHAPTER II
ERROR ANALYSIS

Assuming a purely reactive load, errors in the antenna parameters determined by the scattering technique are attributed to inaccuracies in the recording system and to inaccuracies in the correlation of the echo area to those loads that cause maximum, minimum, and average scattering cross section. Since the error in the predicted value of the scattering cross section for any load is readily determined once the error in the antenna input impedance is known, a method for estimating error in the input impedance of the antenna under test is presented.

The experimental data taken with the programmed load is a calibrated echo-area-versus-load curve from which the loads that cause maximum, minimum, and average scattering cross section are extracted. These loads are plotted on a Smith Chart and the input impedance of the antenna is determined using geometrical constructions (see Appendix B).

If an error in recording echo area exists, it is apparent that a large slope on the σ-versus-load curve would result in a smaller range from which the associated load could be selected. Any error inherent in the load itself would extend the selection range of the load. This is illustrated in Fig. 1. The slope, $\frac{d(\sigma/\sigma_{max})}{d\ell_\lambda}$, is expressed by the

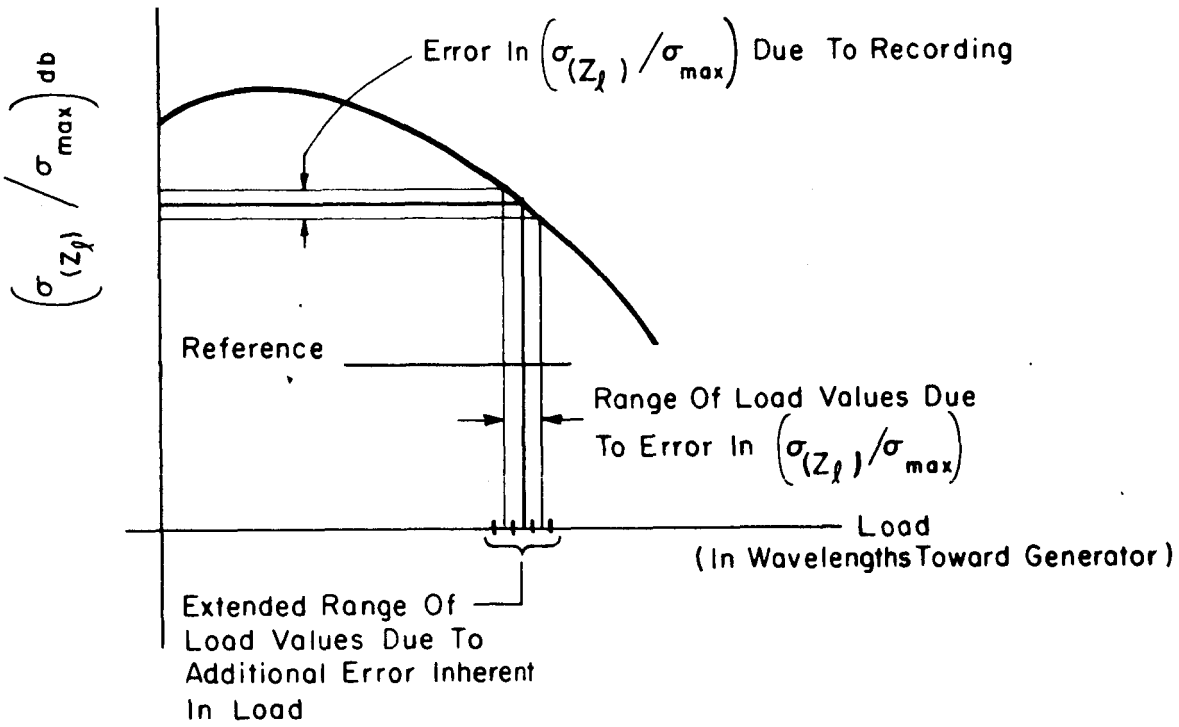

Fig. 1. Selection range of load values resulting from recording and load errors.

equation (developed in Appendix C),

$$(5) \qquad \frac{d(\sigma/\sigma_{max})}{d\ell_\lambda} = \frac{2|C|\,(\cos\phi - 1)\,[\sin(\alpha-\phi)]\,2\pi\,\sec^2 2\pi\ell_\lambda}{[\,|C| + 1]^2\,R_a/Z_{c_2}},$$

where ϕ is the phase of the load-dependent component; R_a/Z_{c_2} is the normalized real part of the antenna impedance; Z_{c_2} is the characteristic impedance of the transmission line connecting the antenna and load; α is the phase of the fixed scattering component; and $\ell_\lambda = \ell/\lambda_g$, where λ_g is the wavelength in the transmission line connecting the

antenna and the load and ℓ is the distance in the transmission line of a movable short from the load terminals. Since α and ϕ are functions of both the antenna impedance, $Z_a = R_a + jX_a$, and the load, the variables of Eq. (5) are inseparable. From Eq. (5) it can be seen that the slope is related to the magnitude and phase relationship between the fixed and load-dependent scattering component, as well as to the antenna resistance.

Referring to Fig. 26 in Appendix B (graphical determination of Z_a^*/Z_{c_2}, the normalized complex conjugate of the antenna impedance) one can see that for a small change in Γ_2, defined by

$$\Gamma_2 = \frac{jX_{\ell_2} - Z_{c_2}}{jX_{\ell_2} + Z_{c_2}} \tag{6}$$

(note that Γ_2 and X_{ℓ_2} are the same point on the Smith Chart since the load X_{ℓ_2} is purely reactive), the distribution of the point Z_a^*/Z_{c_2} is dependent upon the values of Γ_2^{max}, Γ_2^{min}, and Γ_2^{avg}. There are several combinations of loads that cause echo area maximum, minimum, and average that will give the same antenna input impedance. The combination of loads depends upon the magnitude and phase of the fixed scattering component which can be altered by adjustment of the nulling signal, i. e., feeding back a portion of the transmitted signal to combine with the fixed-scattered signal, hence changing the total fixed scattering component. The selection of different combinations of loads will probably result in different distributions of the point

Z_a^*/Z_{c_2} for a given load error. Whether or not there is less spreading of the point Z_a^*/Z_{c_2} will depend upon the recording error and the shape of the new echo-area-versus-load curve. For all possible combinations of Γ_{2s} (having error) and the associated Z_a^*/Z_{c_2}, it is not obvious whether the maximum change in Z_a^*/Z_{c_2} will occur when the Γ_2 values are at their extremes or at some intermediate values.

For a systematic approach to an error analysis, the expressions in Table I defining the antenna impedance in terms of loads that cause maximum, minimum, and average echo area are presented. The development of the expressions in Table I is given in Appendix D. Four cases result but only three loads are necessary to determine Z_a.

For all cases the antenna resistance can be expressed as

$$R_a = \frac{BH}{1 + H^2} \tag{7}$$

and the antenna reactance as

$$X_a = -b + \frac{BH^2}{1 + H^2} = -c - \frac{B}{1 + H^2} , \tag{8}$$

where H is of the form

$$H = \frac{1 - b/a}{1 - c/a} , \tag{9}$$

and a, b, c, and B are defined in Table I. Substituting Eq. (7) into Eq. (8),

(10) $$X_a = -b + R_aH = -c - R_a/H.$$

From the total differential of Eqs. (7) and (10) we have

(11) $$\frac{dR_a}{R_a} = \frac{dB}{B} + \left(\frac{B - 2R_a}{B}\right) \frac{dH}{H} ,$$

and

(12) $$dX_a = \frac{R_a}{H^2} dH - \frac{dR_a}{H} - dc,$$

or

(13) $$\frac{dX_a}{X_a} = - \frac{R_a/H}{R_a + cH} dH + \frac{dR_a}{R_a + cH} + \frac{H}{R_a + cH} dc,$$

where

(14) $$dB = db - dc,$$

and

(15) $$\frac{dH}{H} = \frac{1}{a-c} \left(-da - \frac{db}{H} + dc + \frac{da}{H}\right) .$$

Since c, B, and H are functions of one, two, and three variables, respectively, and the respective changes must also be correlated (dH^{max} and dB^{max} may not occur at the same time), an analytical approach is quite involved and a graphical analysis seems to offer the best solution. Since the equations defining R_a/Z_{c_2} and X_a/Z_{c_2} (Eqs. (7), (8), and (9)) have a form independent of what three loads out of four are selected to determine R_a/Z_{c_2} and X_a/Z_{c_2}, the distribution in the antenna input impedance could be determined by a computer

over a range of load values due to error of each particular load. In general, the basic Eqs. (7), (8), and (9) would be programmed and the range of the load values would appear as input data.

TABLE I

R_a and X_a as functions of loads that cause maximum, minimum, and average scattering cross section

	Case 1	Case 2	Case 3	Case 4
Load Selections	$x_l^{avg\ 1}, x_l^{avg\ 2}, x_l^{min}$	$x_l^{max}, x_l^{min}, x_l^{avg\ 2}$	$x_l^{max}, x_l^{min}, x_l^{avg\ 1}$	$x_l^{max}, x_l^{avg\ 1}, x_l^{avg\ 2}$
B	$x_l^{avg\ 1} - x_l^{avg\ 2}$	$x_l^{min} - x_l^{max}$	$x_l^{max} - x_l^{min}$	$x_l^{avg\ 2} - x_l^{avg\ 1}$
H	$\dfrac{x_l^{min} - x_l^{avg\ 1}}{x_l^{min} - x_l^{avg\ 2}}$	$\dfrac{x_l^{avg\ 2} - x_l^{min}}{x_l^{avg\ 2} - x_l^{max}}$	$\dfrac{x_l^{avg\ 1} - x_l^{max}}{x_l^{avg\ 1} - x_l^{min}}$	$\dfrac{x_l^{max} - x_l^{avg\ 2}}{x_l^{max} - x_l^{avg\ 1}}$
b	$x_l^{avg\ 1}$	x_l^{min}	x_l^{max}	$x_l^{avg\ 2}$
c	$x_l^{avg\ 2}$	x_l^{max}	x_l^{min}	$x_l^{avg\ 1}$
a	x_l^{min}	$x_l^{avg\ 2}$	$x_l^{avg\ 1}$	x_l^{max}

For employment of the graphical technique, general graphs of Eqs. (7), (9), and (10) are presented in Figs. 2-8 for $-5 \leq H \leq 5$, $R_a \leq 3.6$, and $-7.6 \leq (X_a + b) \leq 7.6$. Since the antenna input impedance can be rotated around the Smith Chart by simply adding a length of line, and the structural or fixed component of the scattering signal can be readily altered, it is likely that Figs. 2-8 can be used for the majority of practical cases.

For a typical illustration consider the case in which the loads that cause maximum, minimum, and average scattering cross section are $-1.065 \leq X_\ell^{min} = -1 < -0.933$, $0.462 \leq X_\ell^{avg\ 2} = 0.5 < 0.538$, and $1.85 \leq X_\ell^{avg\ 1} = 2 < 2.164$. An error of $\pm 0.005\lambda$ is assumed in positioning the loads. The variation in H is found by plotting the maximum variation in c/a, b/a, and c/b (Fig. 2). Similarly, the variation in R_a and $X_a + X_\ell^{avg\ 1}$ or X_a are found (see Figs. 6 and 8, area A) and transferred to Fig. 16, area A.

Since the impedance does not vary linearly with distance on the Smith Chart, reading accuracy may be optimized by having the antenna input impedance fall in the vicinity of real $Z_a < 1$ on the Smith Chart. The impedance could easily be rotated to this vicinity by adding a length of transmission line to the scattering antenna terminals.

The formulas in Eqs. (7) and (10) can be reduced to

$$R_a = \frac{B}{H} \tag{16}$$

and

$$X_a = -c - \frac{B}{H^2} \tag{17}$$

for large values of H. For values of $H > 5$ in Eq. (7), an error of 0.75% in R_a will result because of the approximation in using Eq. (16).

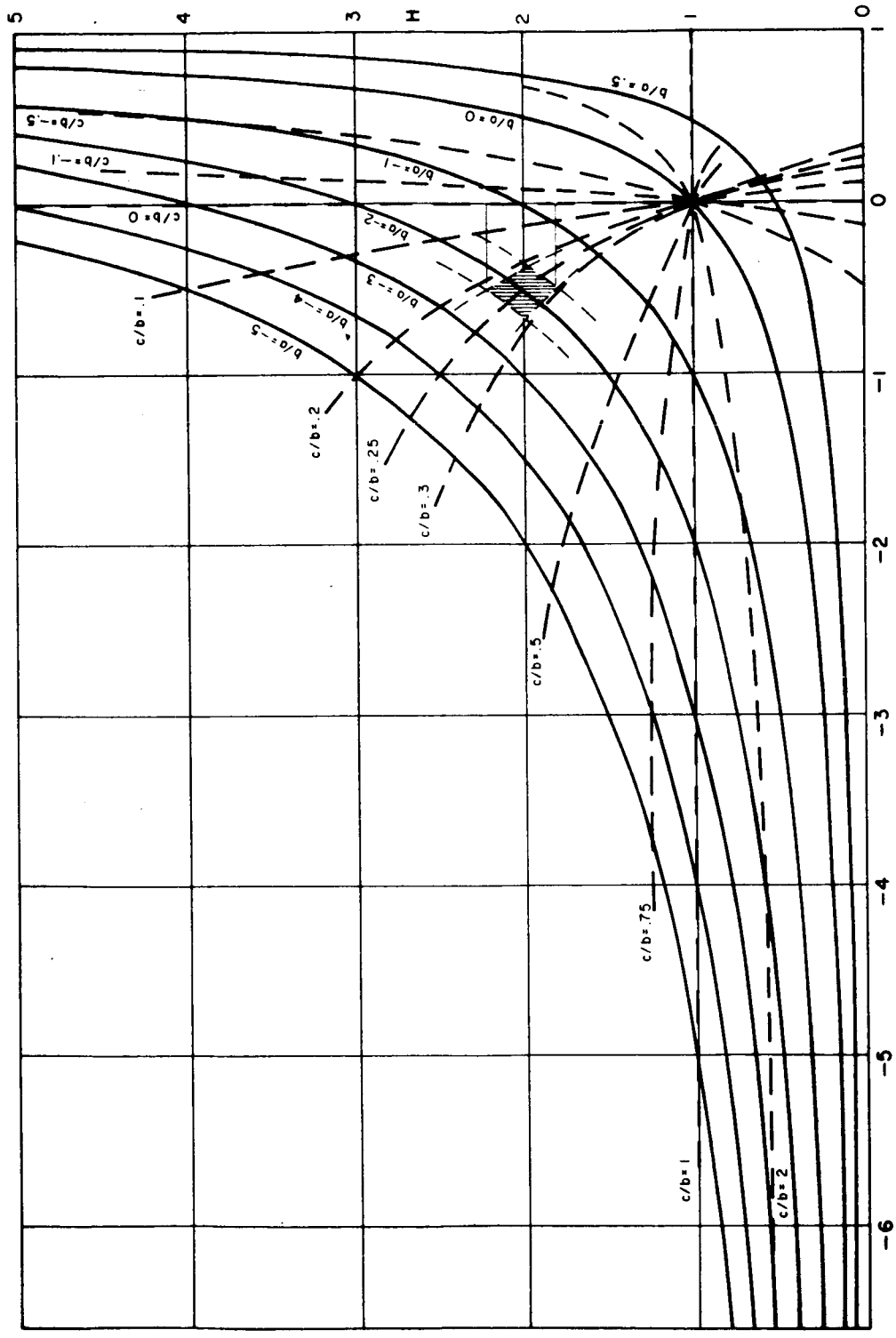

Fig. 2. H = 1-b/a/1-c/a curves for $c/a \leq 1$ and $H \geq 0$.

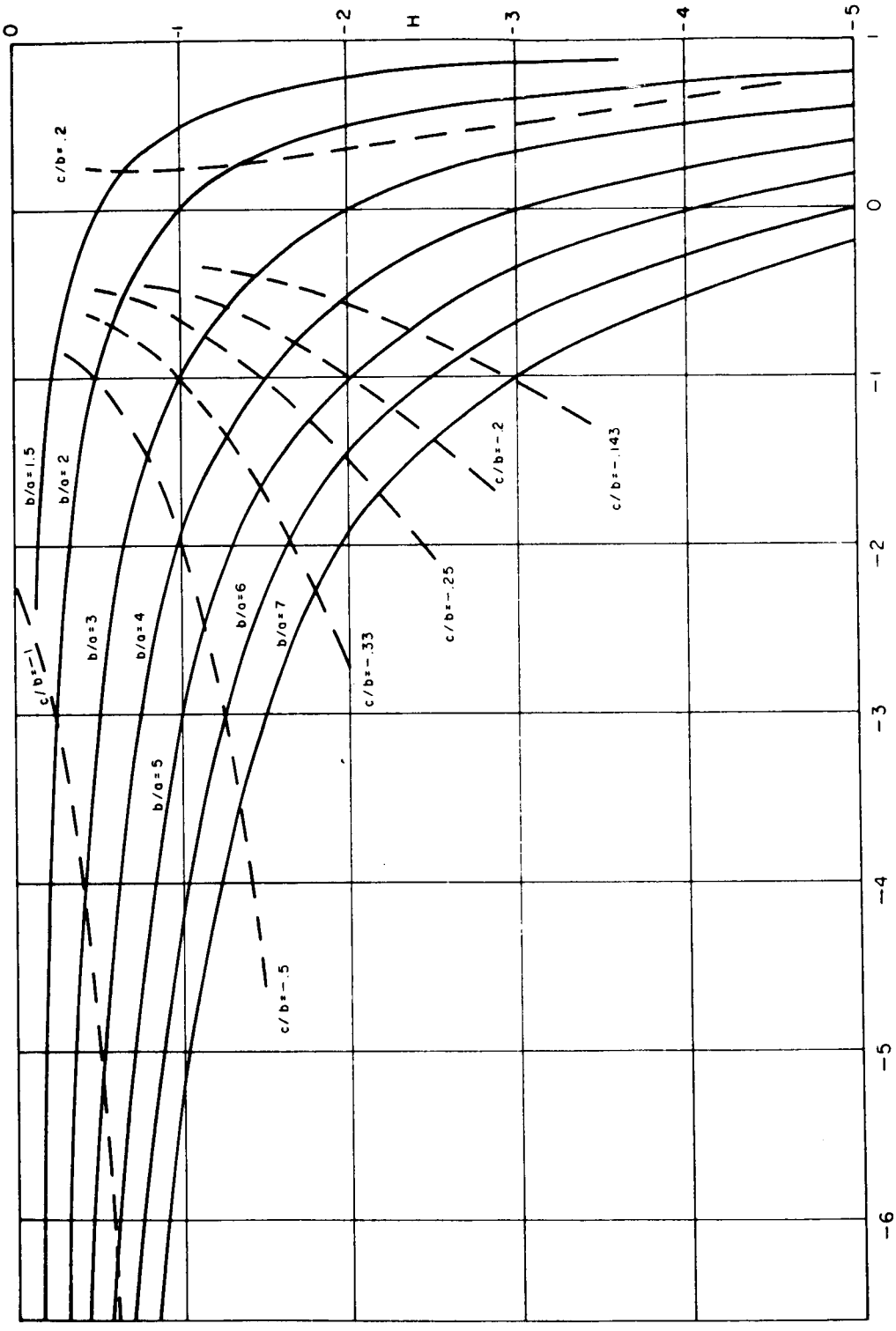

Fig. 3. $H = 1-b/a/1-c/a$ curves for $c/a \leq 1$ and $H \leq 0$.

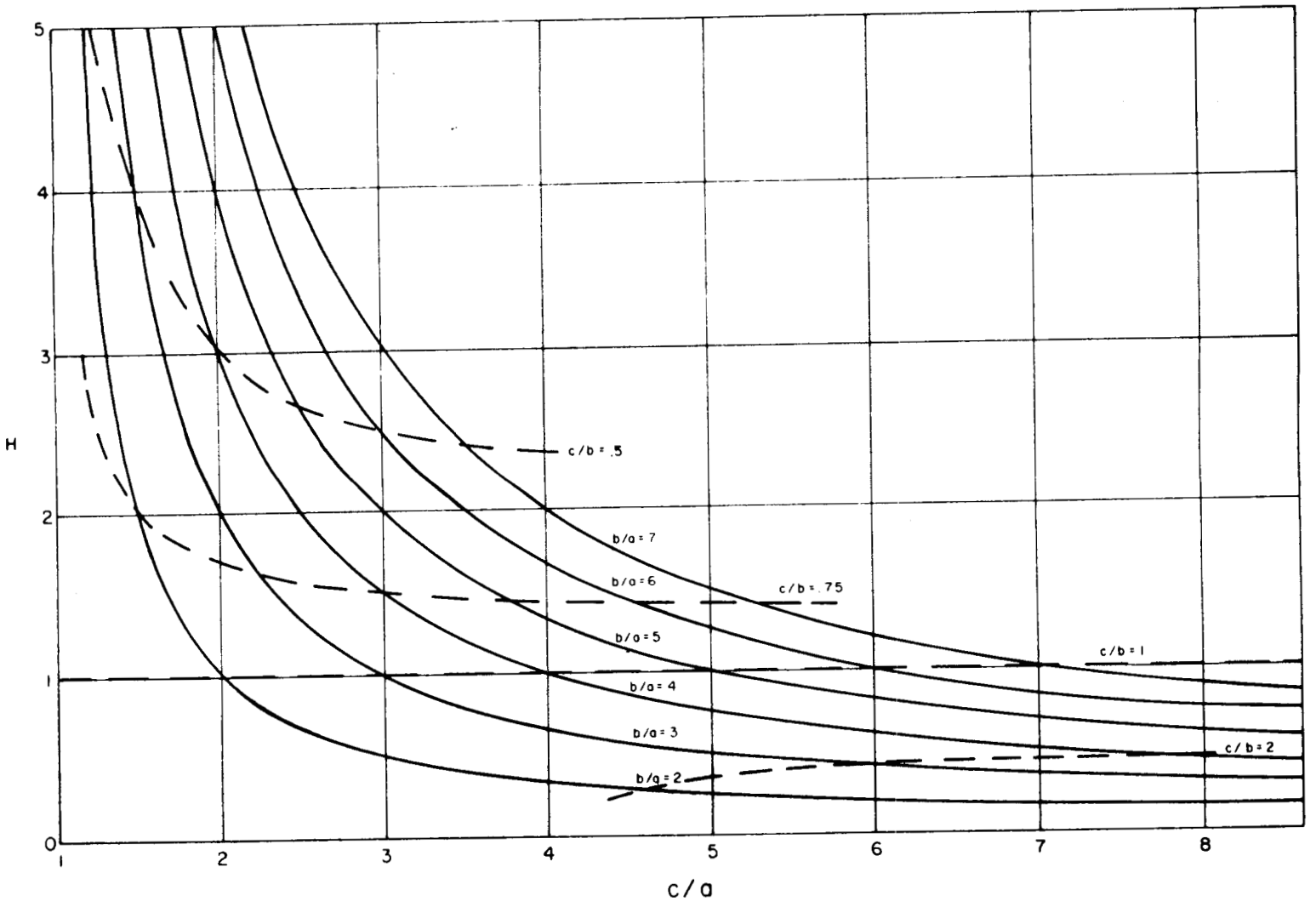

Fig. 4. $H = 1-b/a \,/\, 1-c/a$ curves for $c/a \geq 1$ and $H \geq 0$.

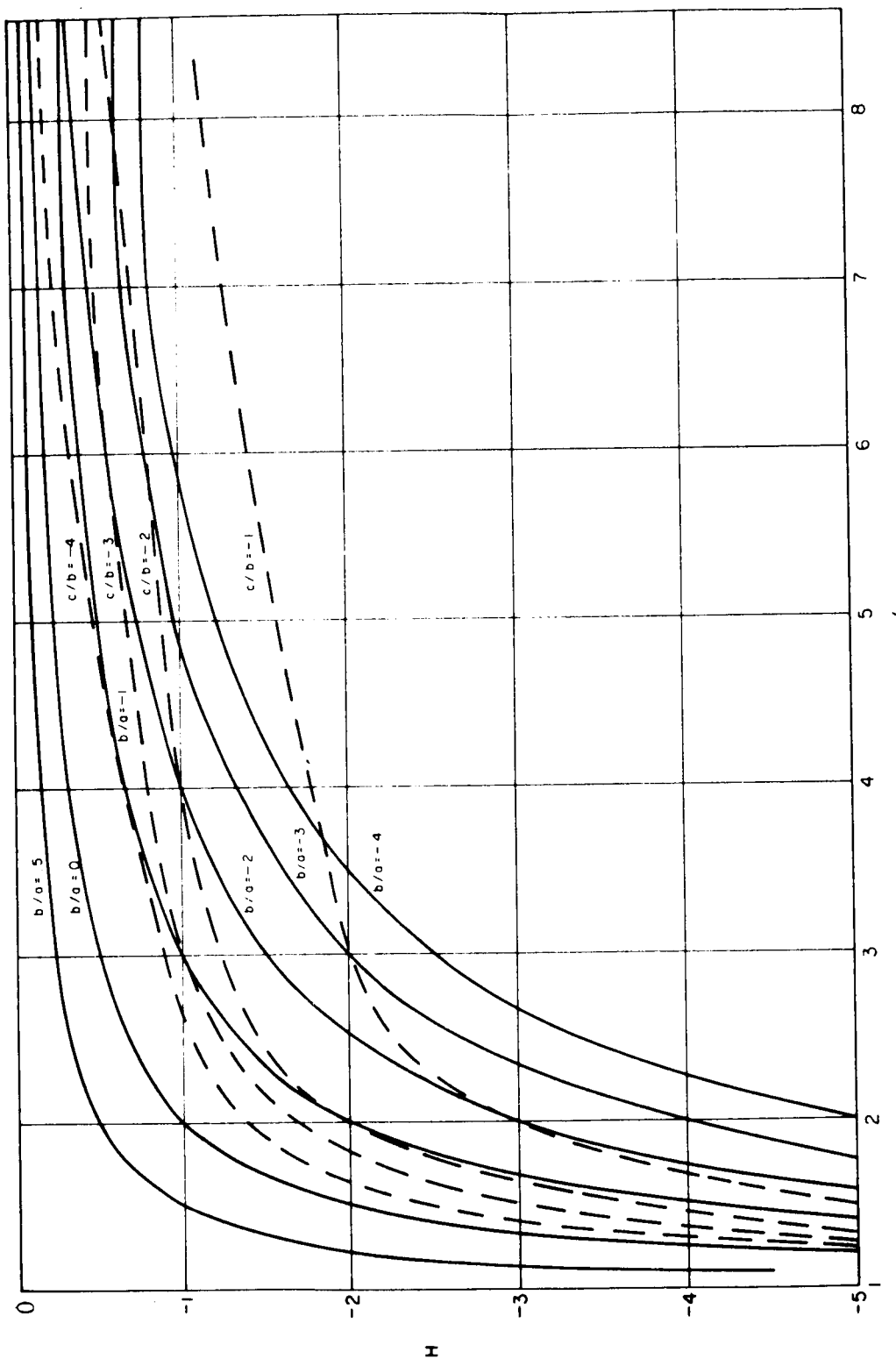

Fig. 5. $H = 1-b/a/1-c/a$ curves for $c/a \geq 1$ and $H \leq 0$.

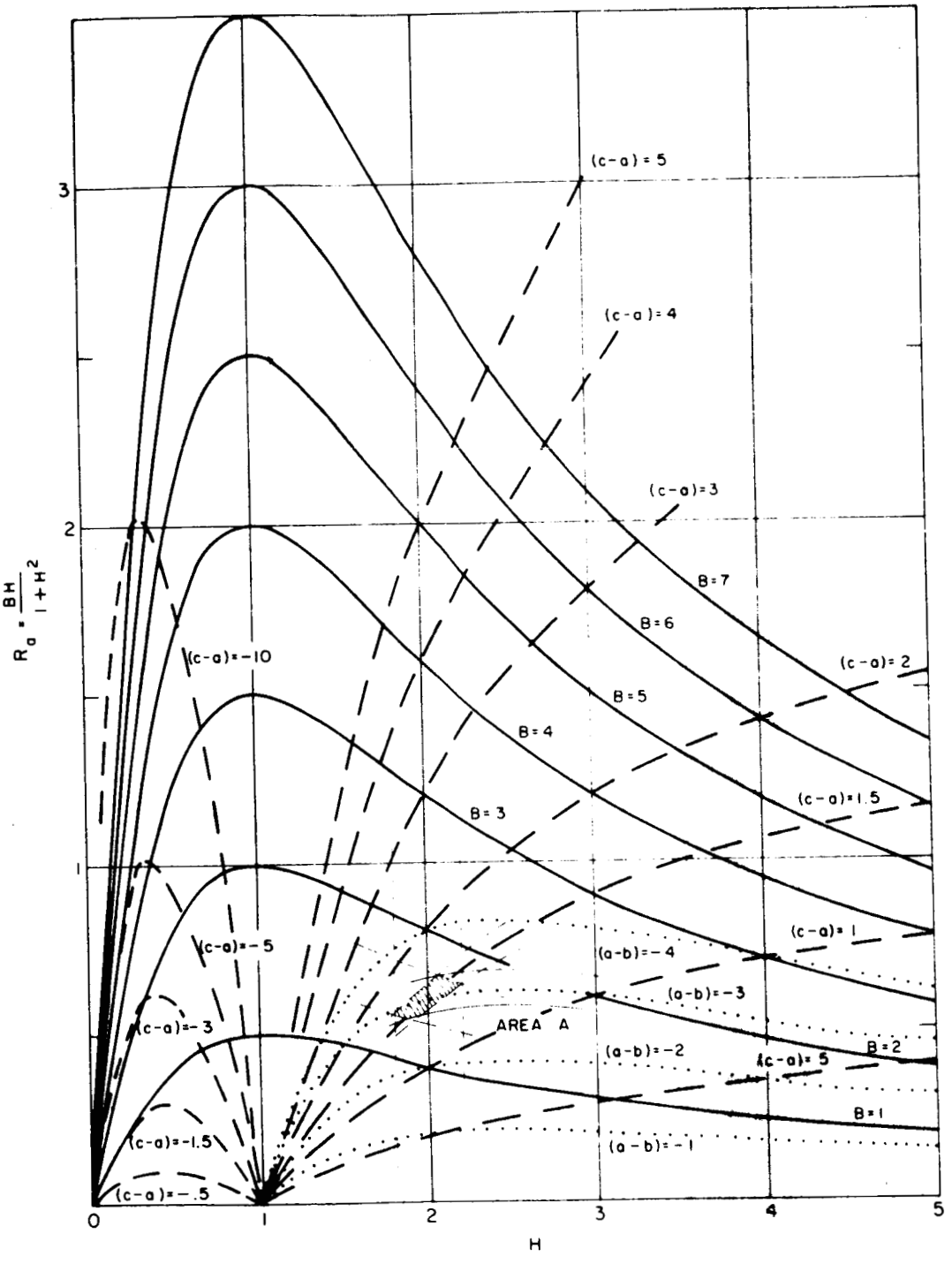

Fig. 6. $R_a = f(B, H, c-a, a-b)$ curves for $R_a \leq 3.6$ and $H \leq 5$.

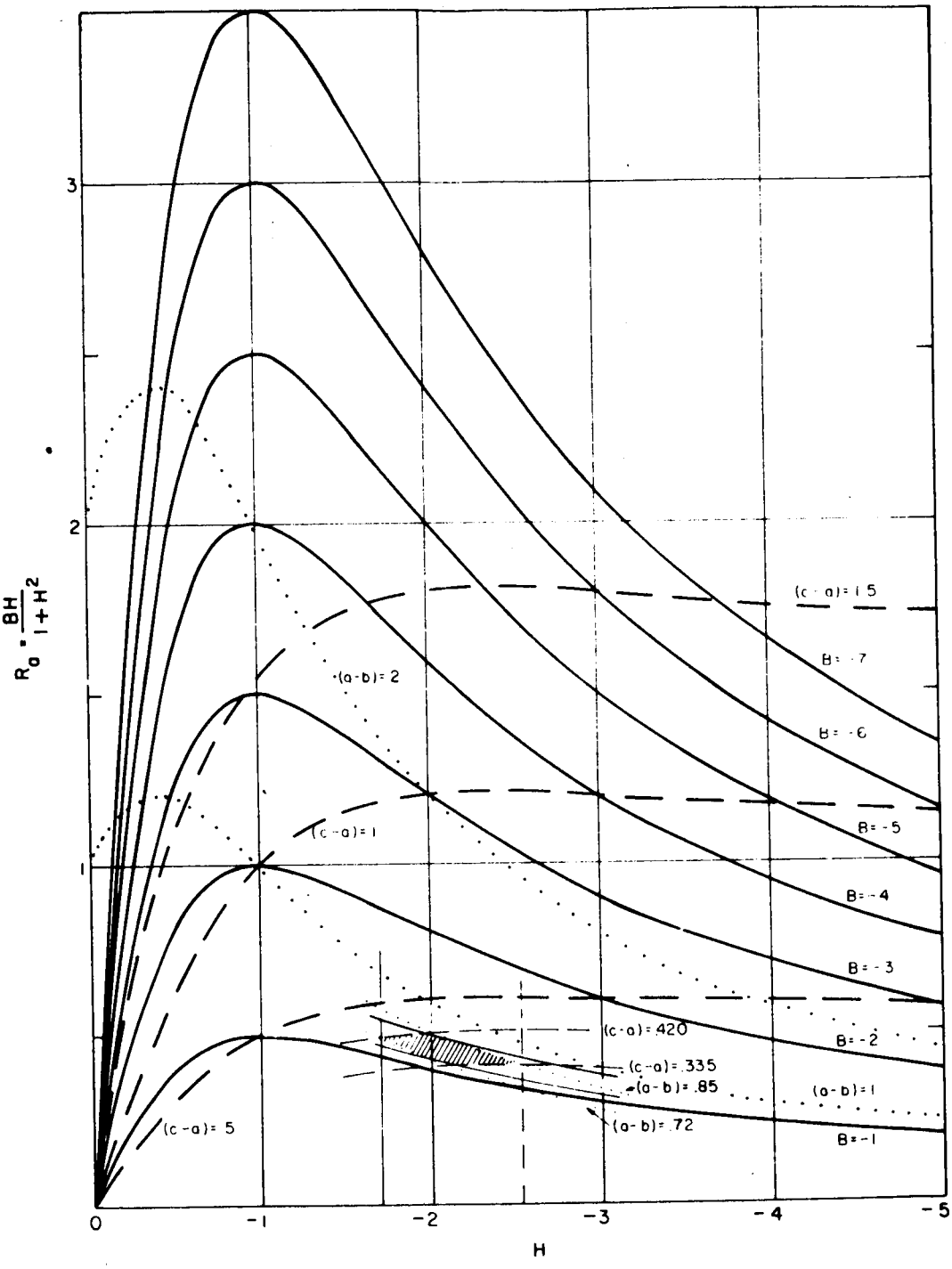

Fig. 7. $R_a = f(B, H, c\text{-}a, a\text{-}b)$ curves for $R_a \leq 3.6$ and $H \geq -5$.

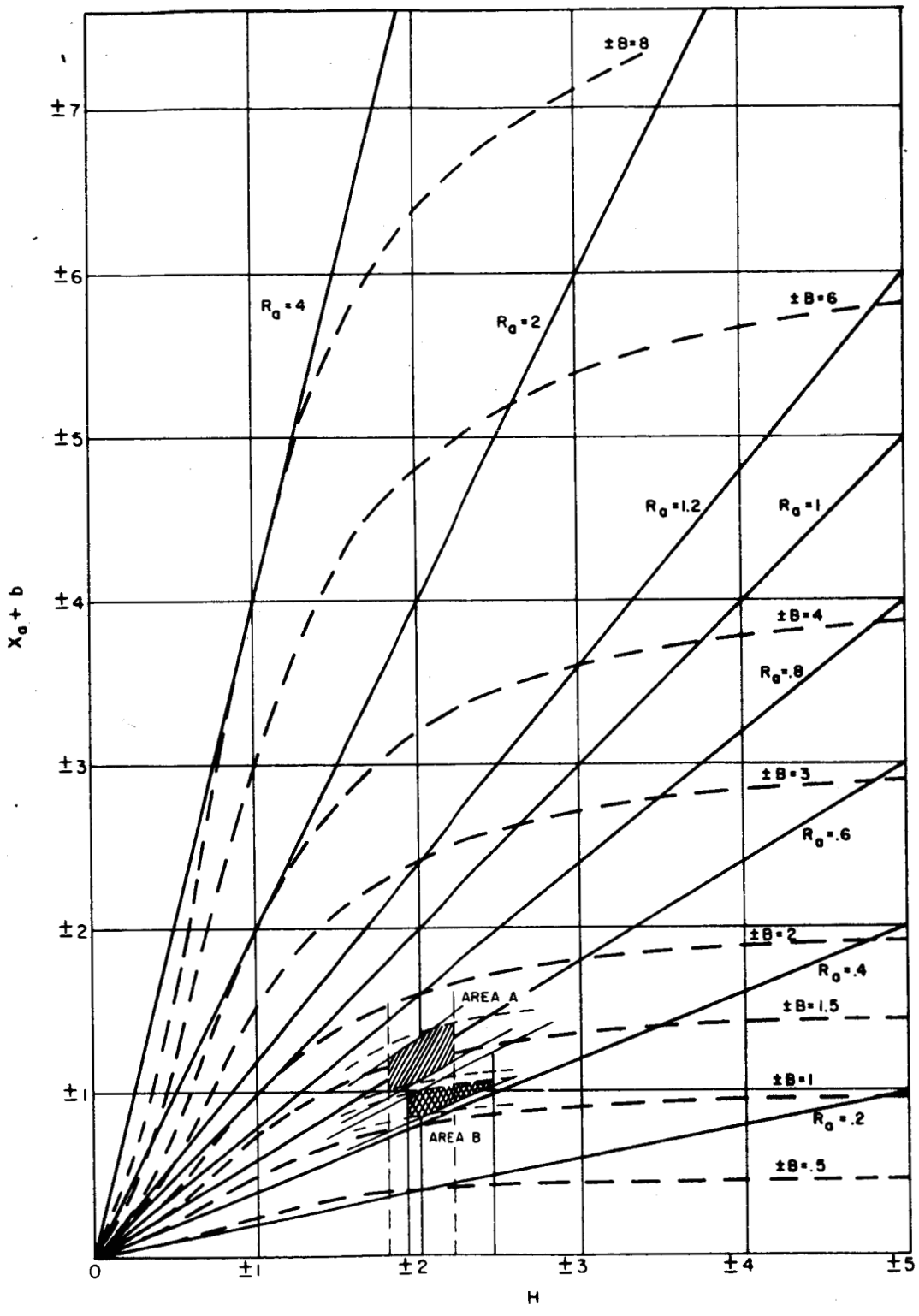

Fig. 8. $X_a + b = f(R_a, H, B)$ curves for $|X_a + b| \leq 7.6$ and $|H| \leq 5$.

CHAPTER III
PROGRAMMED LOAD

A block diagram of the programmed load and its electrical reversing network are shown in Fig. 9. Photographs of the programmed load with X-band guide and of the coaxial load attachment are shown in Fig. 10. The programmed load is a movable choke short driven by a d-c motor. The system employs a cam-operated switch to electrically reverse the direction of the short and also employs cam-operated stubs spaced $\lambda_g/4$ apart which disturb the fields in the waveguide every 1/72 inch movement of the short. This disturbance appears as a spike on the pattern which enables echo area and load to be correlated.

The accuracy of the position of the short was found to be within $\pm 0.0025\lambda_g$ at $\lambda_g = 4$ cm.

The only difficulty encountered in using the programmed load was caused by erratic operation of the reversal switch by the slow-moving cam. The push-button switches that were used would occasionally not trip at precisely the same point when activated very slowly, hence losing calibration. A specially designed switch or quicker means of activating typical push-button switches is recommended to improve the performance of the programmed load.

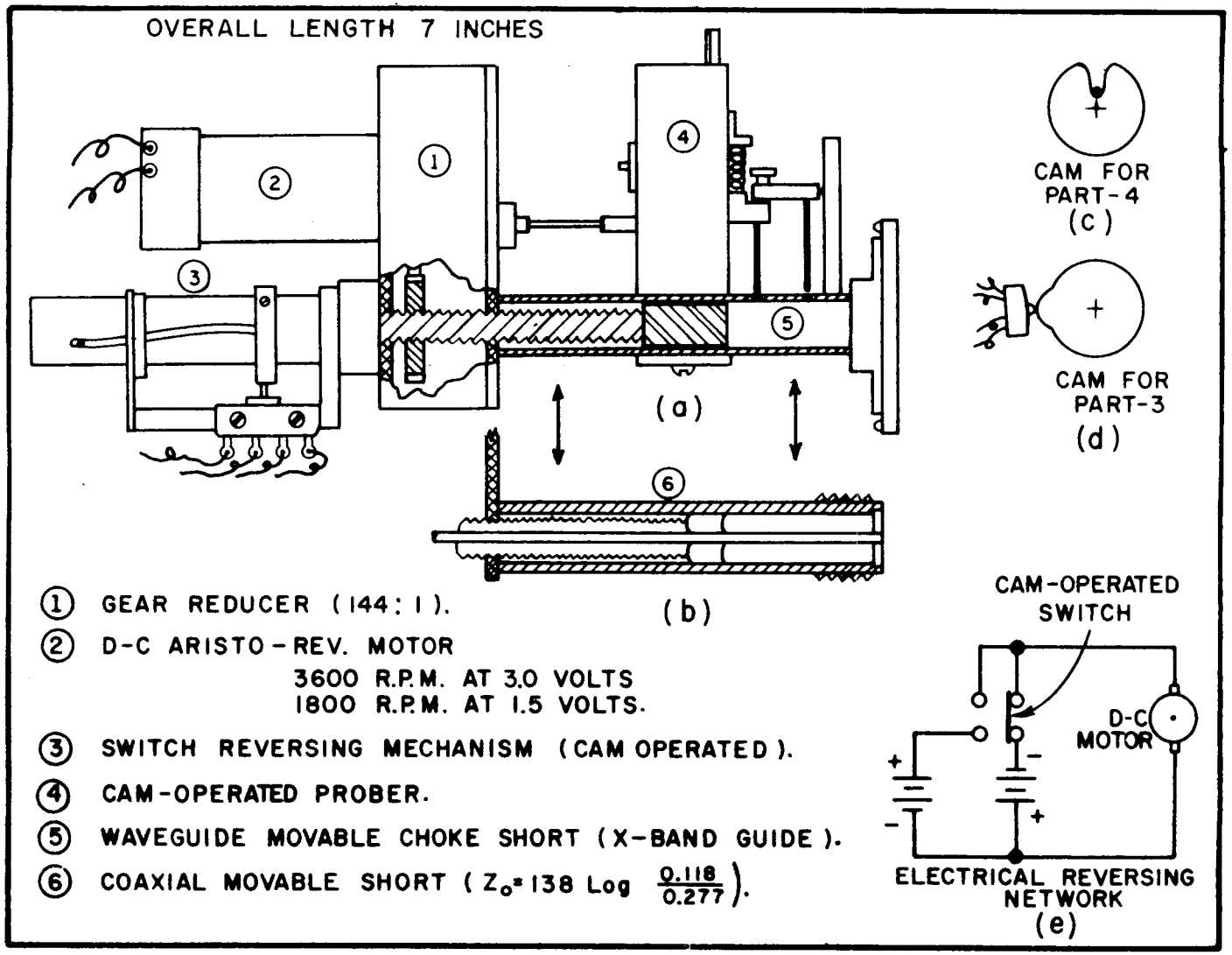

Fig. 9. Block diagram and electrical network of programmed load.

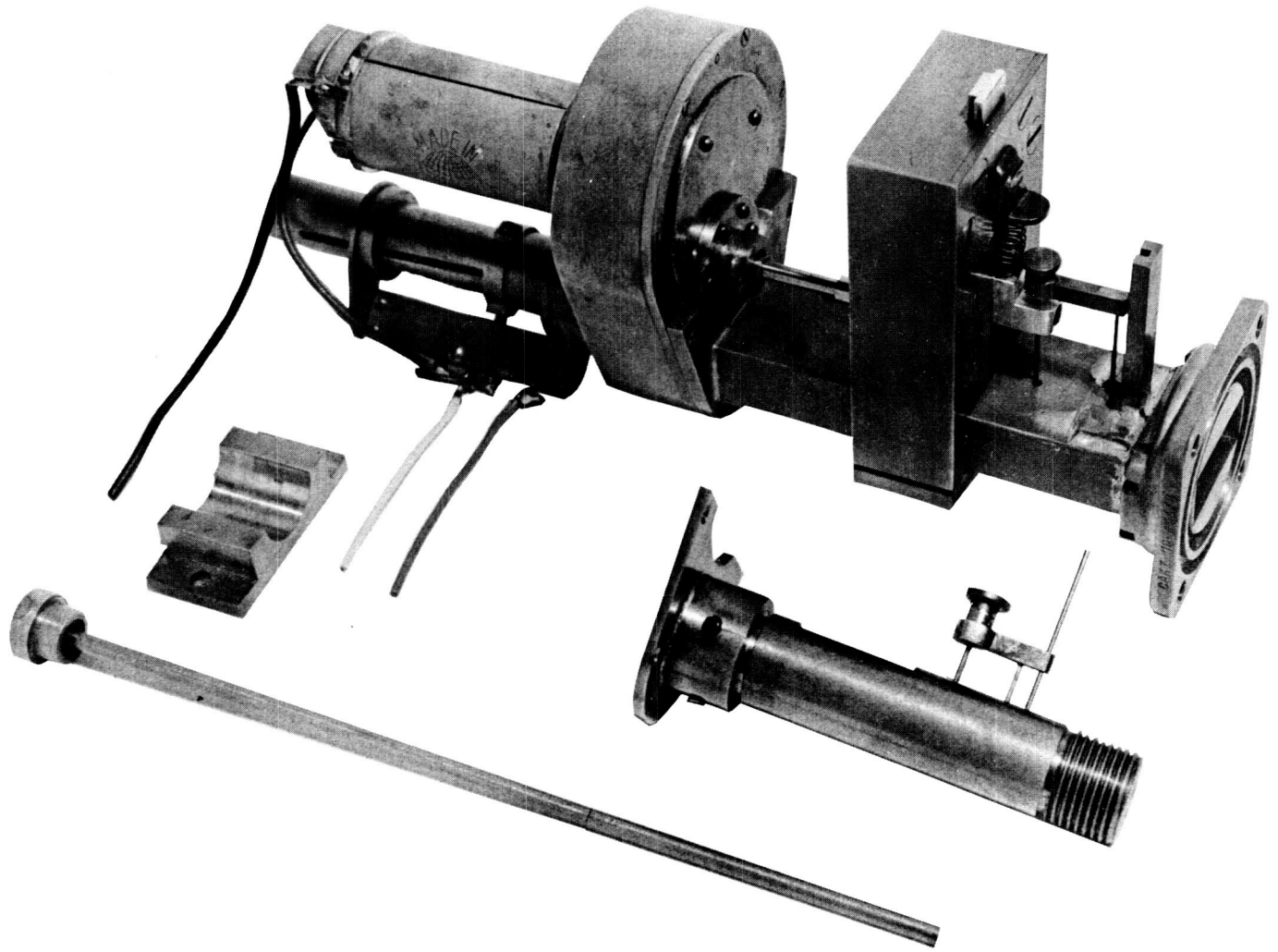

Fig. 10. Photograph of programmed load, X-band load and coaxial load attachment shown separately.

CHAPTER IV
A NON-PROGRAMMED LOAD ANALYSIS

In earlier work, [1, 4, 5] the method for determining input impedance, gain, and echo area of an antenna from amplitude-scattering measurements requires the use of a continuous, calibrated, variable-reactive load and a means of signaling to the operator the position of the load at a given time. It is shown in this section that a load consisting of a reversible short in a transmission line that varies from 0λ to 0.75λ on a Smith Chart can also be employed without any signaling provision.

Assuming that any change in the nulling signal does not affect the power density at the target, we consider four cases employing a variable short-to-open-circuit load. These four cases are not unique but they are sufficient for determining gain, impedance, and echo area. In three cases the nulling signal is adjusted for zero echo area when the load at the antenna terminals is initially at a short-circuit, an open-circuit, and some preset load other than open-circuit or short circuit, respectively. In the fourth case the nulling signal is adjusted for zero echo area with no target (nulled system). From Case 1 or Case 2 the ratio $\pm R_a/X_a$ can be found. From Case 3 possible values of R_a/Z_{c_2} and $\pm X_a/Z_{c_2}$ can be found and the correct values selected by using the information from Case 1

or Case 2. Case 4 is necessary if the scattering from an antenna for any load is to be predicted. Possible values of R_a/Z_{c_2} and X_a/Z_{c_2} can also be found using the method of Case 4 and the correct values selected by using the information from Case 1, 2, or 3. Because of more complexity in determining Z_a by Case 4 and that Case 1, 2, or 3 is necessary to determine the correct value of gain, it is suggested that the input impedance of the antenna be determined by Case 3 in conjunction with Case 1 or Case 2 and that Case 4 be used to determine the magnitude and phase of the fixed scattering component of the antenna in order that the echo area for any load could be predicted.

The basic formulas of the scattering method are repeated here for the convenience of the reader.

(18) $$\sigma = \kappa \left|\Gamma_1\right|^2$$

(19) $$\frac{\Gamma_1}{B} = C + \Gamma_m$$

(20) $$\Gamma_m = \frac{Z_\ell - Z_a^*}{Z_\ell + Z_a}$$

(21) $$C = \left|C\right| \ (\cos \alpha + j \sin \alpha)$$

(22) $$\left|\frac{\Gamma_1}{B}\right|^2 = CC^* + \Gamma_m^* C + C^* \Gamma_m + 1$$

$$(23) \qquad \left|\frac{\Gamma_1}{B}\right|^2_{Z_\ell=0} = CC^* + 1 - |C| \frac{2R_a^2 \cos\alpha - 4X_aR_a \sin\alpha - 2X_a^2 \cos\alpha}{R_a^2 + X_a^2}$$

$$(24) \qquad \left|\frac{\Gamma_1}{B}\right|^2_{Z_\ell=\infty} = CC^* + 1 + 2|C| \cos\alpha$$

The curves in Fig. 11(a, b, c, d) with the conditions specified respectively in each of the following cases were calculated for an antenna having an input impedance $Z_a = 1.2 + j0.8$ and a fixed scattering component $C = 1.5\angle 60°$ to assist in deriving the non-programmed load technique and also to serve as an example.

Case 1

In Case 1 the nulling signal is adjusted for zero echo area with the load at the antenna terminals initially set at a short-circuit. For this case the calculated echo-area-versus-load curve is shown in Fig. 11a.

From Eq. (24) and normalizing to $|\Gamma_1/B|^{2\,max} = 4$ ($|\Gamma_1/B|^{max} = 2$ since the Smith Chart radius is assumed to be 1),

$$(25) \qquad \frac{\sigma]_{Z_\ell=\infty}}{\sigma_{max}} = \frac{|\Gamma_1/B|^2_{Z_\ell=\infty}}{|\Gamma_1/B|^{2\,max}} = G = \frac{1 + \cos\alpha}{2} \quad .$$

Solving for $\cos\alpha$ we obtain

$$(26) \qquad \cos\alpha = 2G - 1.$$

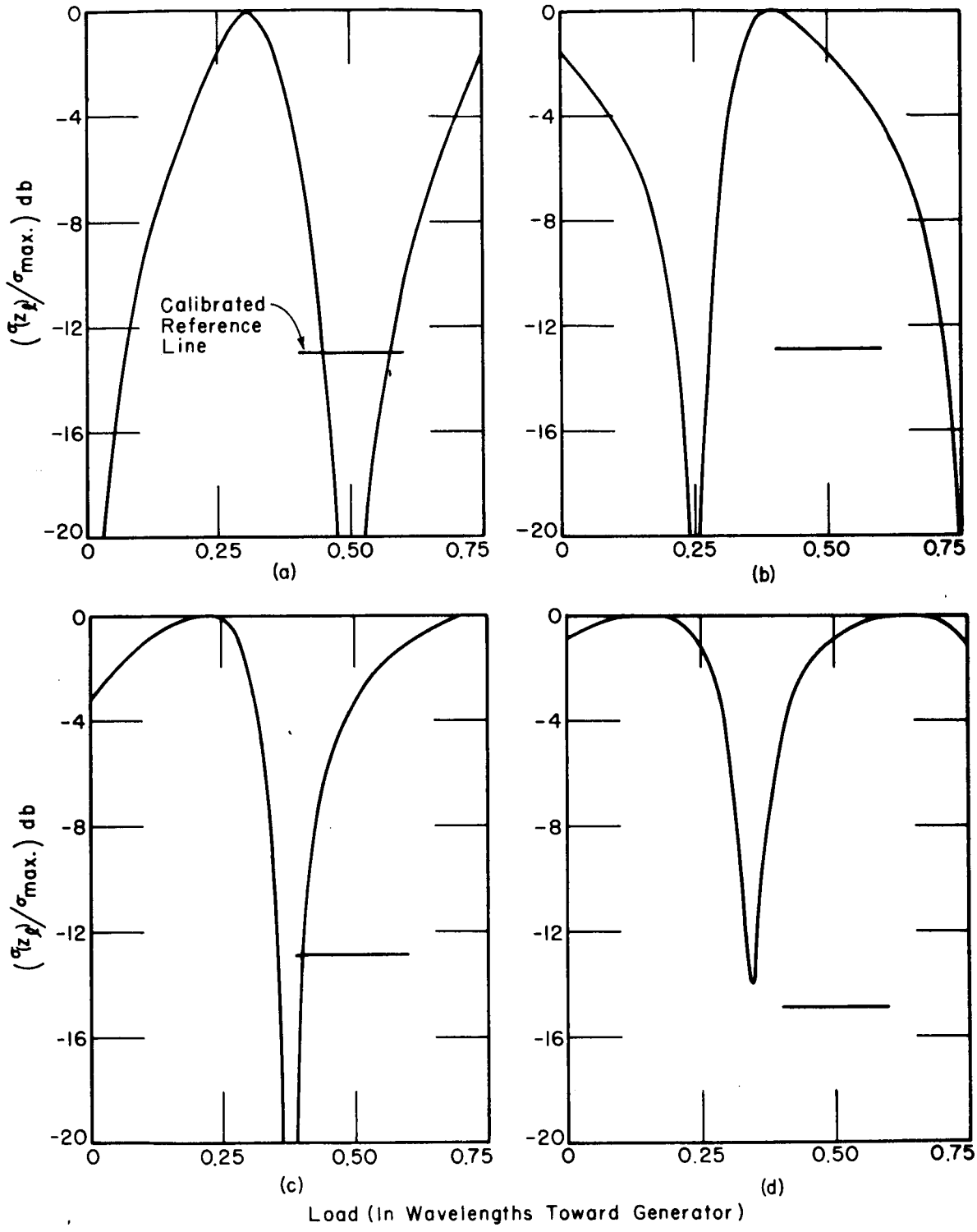

Fig. 11. Calculated echo area versus load with nulling system adjusted for (a) zero echo area at a load of 0λ toward the generator, (b) zero echo area at a load of 0.25λ toward the generator, (c) zero echo area at a load of 0.375λ toward the generator, and (d) a nulled system.

With $\sigma]_{Z_\ell = 0}$ we have

$$(27) \qquad \Gamma_m = -C = -\frac{Z_a^*}{Z_a} = -(\cos\alpha + j\sin\alpha) = \frac{-R_a + jX_a}{R_a + jX_a} \quad .$$

Equating real or imaginary parts of Eq. (27) and making use of Eq. (26),

$$(28) \qquad \frac{R_a^2}{X_a^2} = \frac{\sin^2\alpha}{(\cos\alpha - 1)^2} = \frac{G}{1 - G} \quad .$$

The development is made clearer when the same results are obtained graphically. Assuming the Smith Chart to have a unit radius,

$$(29) \qquad \left|\frac{\Gamma_1(Z_\ell)}{B}\right| = 2\sqrt{\frac{\sigma(Z_\ell)}{\sigma_{max}}} \quad .$$

From the relationship in Eq. (19), $|C| = 1$, and $\Gamma_m]_{Z_\ell = \infty} = 1\angle 0°$, the tail of the phasor, $\Gamma_1/B]_{Z_\ell = \infty}$, will intersect the rim of the Smith Chart at either point a or b Fig. (12). The phasor C is either ao or bo ($\Gamma_m]_{Z_\ell = 0}$ must equal -C for zero cross section). Hence,

$$(30) \qquad \Gamma_m]_{Z_\ell = 0} = -C = 1\angle \pm\alpha = -\frac{Z_a^*}{Z_a} \quad ,$$

which is the same as Eq. (27).

Case 2

In Case 2 the nulling signal is adjusted for zero echo area with the load at the antenna terminals initially set at an open-circuit. For this case the calculated echo-area-versus-load curve is shown in Fig. 11b. Since $\Gamma_m]_{Z_\ell=\infty}=1$ and $|\Gamma_1/B|_{Z_\ell=\infty}=0$, C is equal to $-1\angle 0°$. Substituting C = -1 into Eq. (22) and normalizing to $|\Gamma_1/B|^{2\,max}$,

$$(31) \qquad \frac{|\Gamma_1/B|^2_{Z_\ell=0}}{|\Gamma_1/B|^{2\,max}} = G_1 = \frac{2 - \Gamma_m^* - \Gamma_m}{2} \quad .$$

From Eq. (31) we obtain

$$(32) \qquad \frac{R_a^2}{X_a^2} = \frac{G_1}{1 - G_1} \quad ,$$

where G_1 = G in Eq. (28).

Graphically, Case 2 has the same geometrical construction as Case 1 (Fig. 12) except that the phasor $\Gamma_m]_{Z_\ell=\infty}$ and C or C' are interchanged.

Case 3

In Case 3 the nulling system is adjusted for zero echo area with the load at the scattering antenna terminals initially preset at a value other than open-circuit or short-circuit load. For a preset purely reactive load of 0.375λ (-j1) towards the generator, the calculated echo-area-versus-load curve is shown in Fig. 11c.

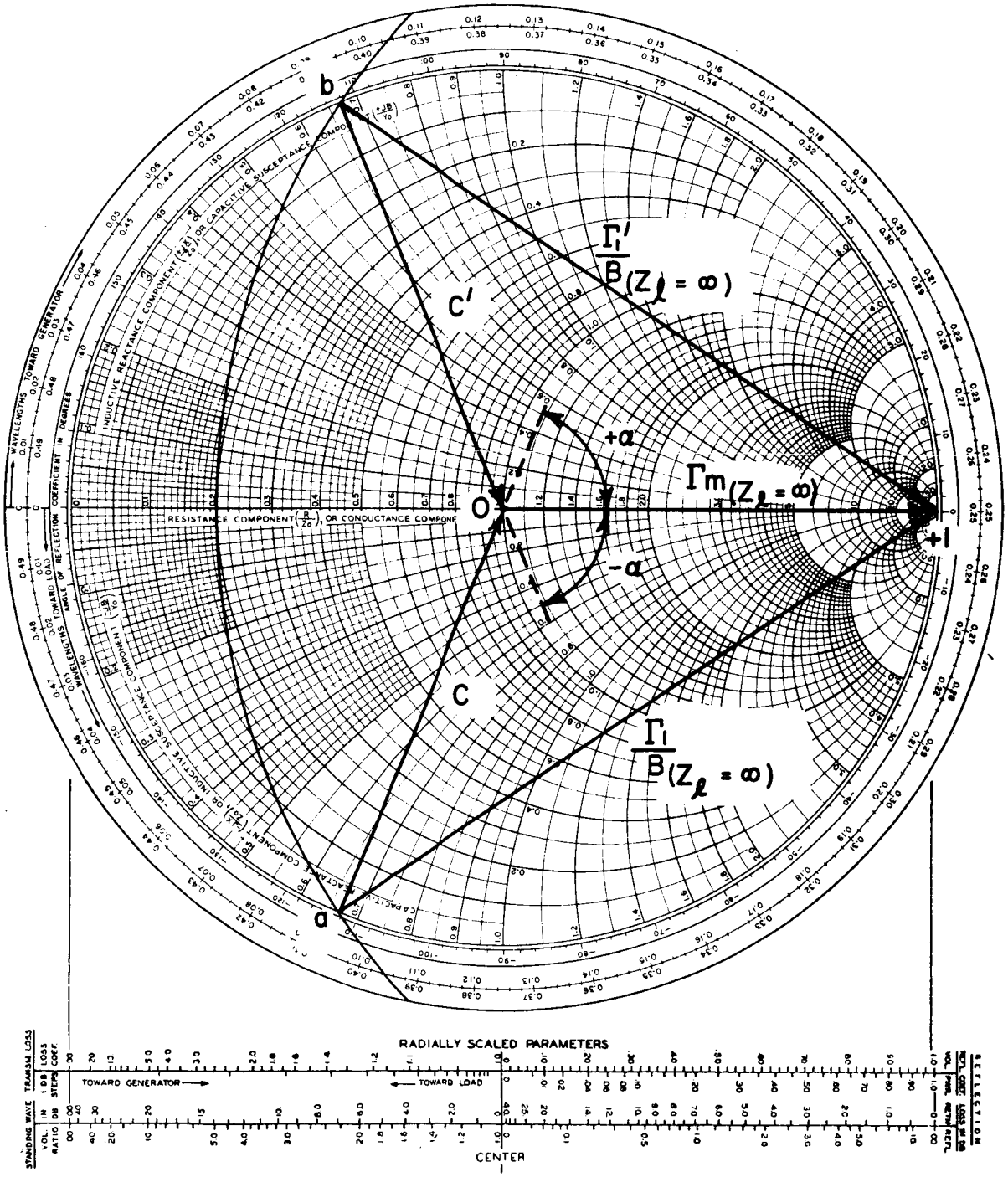

Fig. 12. Graphical solution for case where nulling signal was adjusted for zero echo area at a load of 0λ toward the generator (Case 1).

Then from Eqs. (20) and (21)

$$(33) \qquad \Gamma_m\Big]_{Z_\ell = Z_{\ell_1}} = -C = \frac{Z_{\ell_1} - Z_a^*}{Z_{\ell_1} + Z_a} = -|C|(\cos\alpha_1 + j\sin\alpha_1).$$

Solving Eq. (33) we find that

$$(34) \qquad \frac{R_a}{X_a + X_{\ell_1}} = \pm \frac{\sin\alpha_1}{\cos\alpha_1 - 1} = \pm\sqrt{\frac{G_3}{1 - G_3}} \ .$$

From Eq. (24) and normalizing to $|\Gamma_1/B|^{2\max}$

$$(35) \qquad \frac{|\Gamma_1/B|^2_{Z_\ell = \infty}}{|\Gamma_1/B|^{2\max}} = G_3 = \frac{1 + \cos\alpha_1}{2} \ .$$

Solving for $\cos\alpha_1$,

$$(36) \qquad \cos\alpha_1 = 2G_3 - 1 \ .$$

From Eq. (23) and normalizing to $|\Gamma_1/B|^{2\max}$

$$(37) \qquad \frac{|\Gamma_1/B|^2_{Z_\ell = 0}}{|\Gamma_1/B|^{2\max}} = G_4 = \frac{1}{2} - \frac{R_a^2\cos\alpha_1 - 2X_aR_a\sin\alpha_1 - X_a^2\cos\alpha_1}{2(R_a^2 + X_a^2)} \ ,$$

which leads to

$$(38) \qquad \frac{R_a}{X_a} = \frac{1}{2G_4 - 1 + \cos\alpha_1}\left[\sin\alpha_1 \pm 2\sqrt{G_4(1-G_4)}\right] .$$

Substituting $\cos\alpha_1$ from Eq. (36),

$$(39) \qquad \frac{R_a}{X_a} = \frac{1}{1 - G_3 - G_4}\left[\frac{\sin\alpha_1}{2} \pm \sqrt{G_4(1-G_4)}\right] .$$

Combining Eqs. (34), (36), and (39),

$$(40) \qquad R_a = \frac{\pm X_{\ell_1}}{\frac{1-G_3-G_4}{\sqrt{G_3(1-G_3)} \pm \sqrt{G_4(1-G_4)}} - \sqrt{\frac{1-G_3}{G_3}}} \quad ,$$

and

$$(41) \qquad X_a = \pm R_a \sqrt{\frac{1-G_3}{G_3}} - X_{\ell_1} \, .$$

The use of Eqs. (40) and (41) in conjunction with Eqs. (28) or (32) and the fact that R_a is positive real for a passive antenna eliminates the ambiguity.

The procedure for the graphical solution is to draw an arc having a radius (see Eq. (29)) of $|\Gamma_1/B|_{Z_\ell=\infty}$ with its center at +1 intersecting the rim of the Smith Chart at T_1 and T_1' (Fig. 13). The phasor C is either $T_1 O$ or $T_1' O$ (see Eq. (19)). Using T_1 and T_1' as centers draw arcs having radii $|\Gamma_1/B|_{Z_\ell=0}$ and intersecting the rim of the Smith Chart at T_2', T_3', T_2, and T_3. Then OT_2', OT_3', OT_2, and OT_3 can represent $\Gamma_m]_{Z_\ell=0}$.

Substituting $\Gamma_m]_{Z_\ell=0} = -Z_a^*/Z_a$ into Eq. (20) and solving for Z_a,

$$(42) \qquad Z_a = \frac{Z_\ell(1-\Gamma_m)}{\Gamma_m - \Gamma_m]_{Z_\ell=0}} \, .$$

$\Gamma_m]_{Z_\ell=Z_{\ell_1}} = -C$ since $\sigma]_{Z_\ell=Z_{\ell_1}} = 0$, then

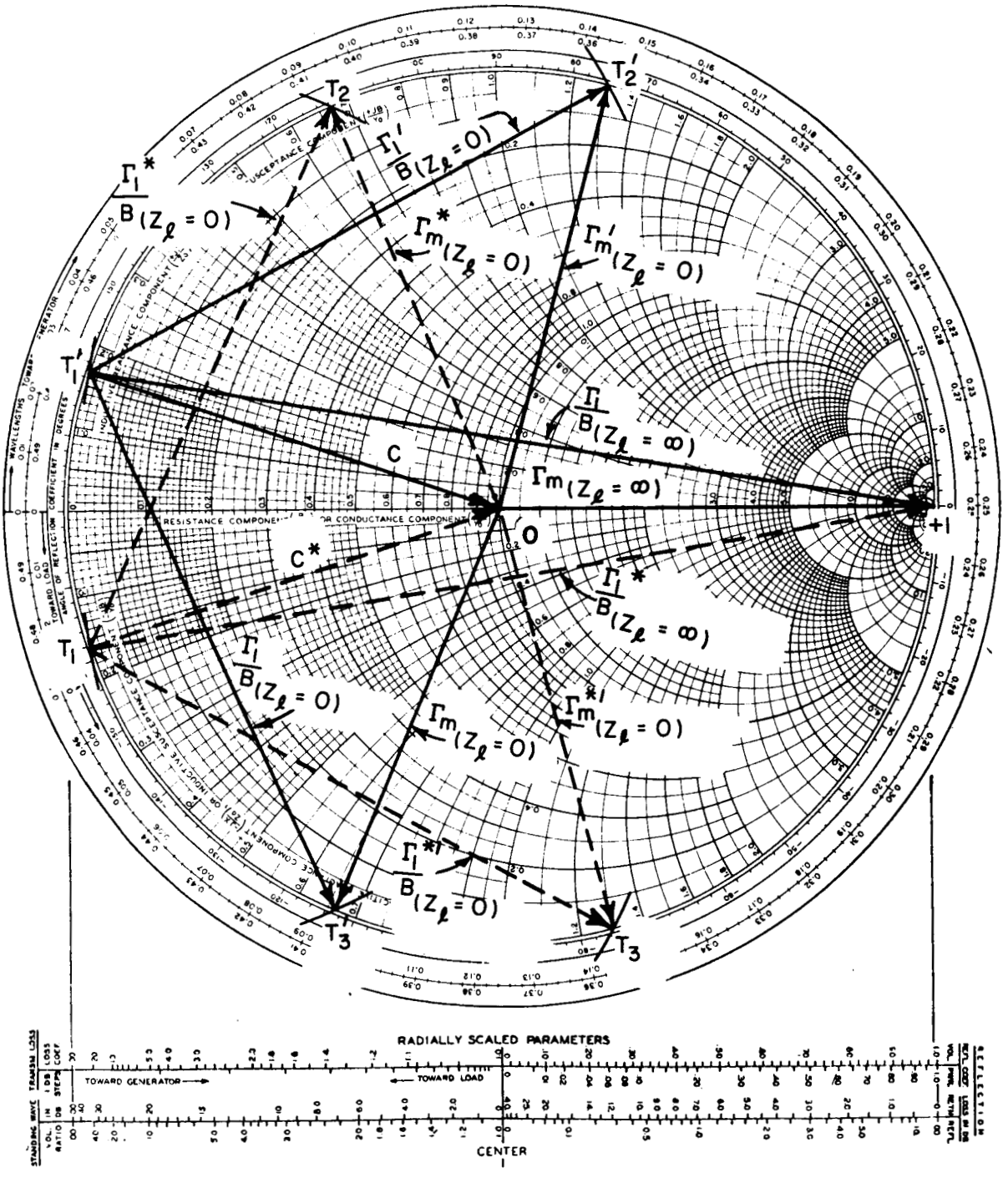

Fig. 13. Graphical solution for case where nulling signal was adjusted for zero echo area at a load of 0.375λ toward the generator (Case 3).

$$(43) \quad Z_a = -\frac{Z_{\ell_1}(1 + C)}{C + \Gamma_m]_{Z_\ell = 0}} \quad ,$$

where the values of C and $\Gamma_m]_{Z_\ell = 0}$ are taken from Fig. 13. There are two sets of combinations: These are C, $\Gamma_m{}']_{Z_\ell = 0}$ and $\Gamma_m]_{Z_\ell = 0}$ and their conjugates. One set is represented by OT_2', OT_3', and OT_1' and the conjugate set by OT_2, OT_3, and OT_1. One set of possibilities is ruled out for a passive antenna since R_a will turn out to be negative.

Assuming $\Gamma_m]_{Z_\ell = 0} = A_o + jB_o$ and $\Gamma_m]_{Z_\ell = Z_{\ell_1}} = A + jB$, we have, using Eq. (42),

$$(44) \quad Z_a = \frac{jX_{\ell_1}(1 - A - jB)}{A + jB - A_o - jB_o} \quad ,$$

which leads to

$$(45) \quad Z_a = \frac{-BX_\ell(A-A_o) + X_\ell(1-A)(B-B_o) + j[X_\ell(1-A)(A-A_o) + BX_\ell(B-B_o)]}{(A - A_o)^2 + (B - B_o)^2} \quad .$$

Using the complex conjugates of $\Gamma_m^*]_{Z_\ell = 0}$ and $\Gamma_m^*]_{Z_\ell = Z_{\ell_1}}$,

$$(46) \quad Z_a = \frac{BX_\ell(A-A_o) - X_\ell(1-A)(B-B_o) + j[X_\ell(1-A)(A-A_o) + BX_\ell(B-B_o)]}{(A-A_o)^2 + (B-B_o)^2} \quad .$$

Since the imaginary components of Eq. (45) and (46) are equal and the real components are opposite in sign, R_a will be negative for one set.

It might be well to note here that the correct value of Z_a may be selected from several possible values of Z_a by comparing the echo area versus load curves constructed using each possible value of Z_a to that measured experimentally. The correct Z_a will be the one that results in the same shape of the measured echo area versus load curve.

Case 4

In this final case, the system is nulled with no target. The calculated echo-area-versus-load curve is shown in Fig. 11d. From Eq. (67) with $p_r p_t = 1$,

$$(47) \qquad |C| = \frac{\pi}{G^2} \frac{(\sigma_{max} - \sigma_{min})}{\lambda^2} ,$$

where G is found using Eq. (66) and Figs. 11a, b, or d. At $Z_\ell = \infty$ (see Eq. (24))

$$(48) \qquad \frac{\sigma]_{Z_\ell = \infty}}{\sigma_{max}} = \frac{|C|^2 + 1 + 2|C| \cos \alpha}{(|C| + 1)^2} = \kappa ,$$

which leads to

$$(49) \qquad \alpha = \pm \arccos \left[\frac{(|C| + 1)^2 \kappa - |C|^2 - 1}{2|C|} \right] .$$

At $Z_\ell = Z_{\ell_1}$ (see Eq. (22))

$$(50) \qquad \frac{\sigma]_{Z_\ell = Z_{\ell_1}}}{\sigma_{max}} = \frac{|C|^2 + 1 + |C| [2 \cos(\alpha - \phi_1)]}{(|C| + 1)^2} = \kappa_1 ,$$

where $\Gamma_m]_{Z_\ell = Z_{\ell_1}} = e^{j\phi_1}$ and $C = |C|\, e^{j\alpha}$. Then

$$(51) \qquad (\alpha - \phi_1) = \pm \arccos\left[\frac{\kappa_1(|C|+1)^2 - |C|^2 - 1}{2|C|}\right].$$

But

$$(52) \qquad \Gamma_m]_{Z_\ell = Z_{\ell_1}} = e^{j\phi_1} = \frac{-R_a + j(X_{\ell_1} + X_a)}{R_a + j(X_{\ell_1} + X_a)},$$

which leads to

$$(53) \qquad \frac{R_a^2}{(X_a + X_{\ell_1})^2} = \frac{\sin^2\phi_1}{(\cos\phi_1 - 1)^2}.$$

Also

$$(54) \qquad \frac{\sigma]_{Z_\ell = 0}}{\sigma_{max}} = \frac{|C|^2 + 1 + 2|C|[\cos(\alpha - \phi_o)]}{(|C|+1)^2} = \kappa_2,$$

where

$$(55) \qquad (\alpha - \phi_o) = \pm \arccos\left[\frac{\kappa_2(|C|+1)^2 - |C|^2 - 1}{2|C|}\right].$$

But

$$(56) \qquad \Gamma_m]_{Z_\ell = 0} = \frac{-R_a + jX_a}{R_a + jX_a} = e^{j\phi_o},$$

which leads to

$$(57) \qquad \frac{R_a^2}{X_a^2} = \frac{\sin^2\phi_o}{(\cos\phi_o - 1)^2}.$$

Solving Eqs. (53) and (57), where ϕ_o and ϕ_1 are determined from Eqs. (49), (51), and (55), leads to the possible solutions of R_a and X_a. The correct values of R_a and X_a are selected using information from Cases 1, 2, or 3.

To obtain the same results graphically, draw a circle with a radius equal to $|C|$ superimposed on a unit circle (Fig. 14, a Smith Chart the radius of which is assumed to be 1). Draw an arc with magnitude

(58) $$r = |\Gamma_1/B|_{Z_\ell=\infty} = \sqrt{\kappa}\ [|C| + 1]$$

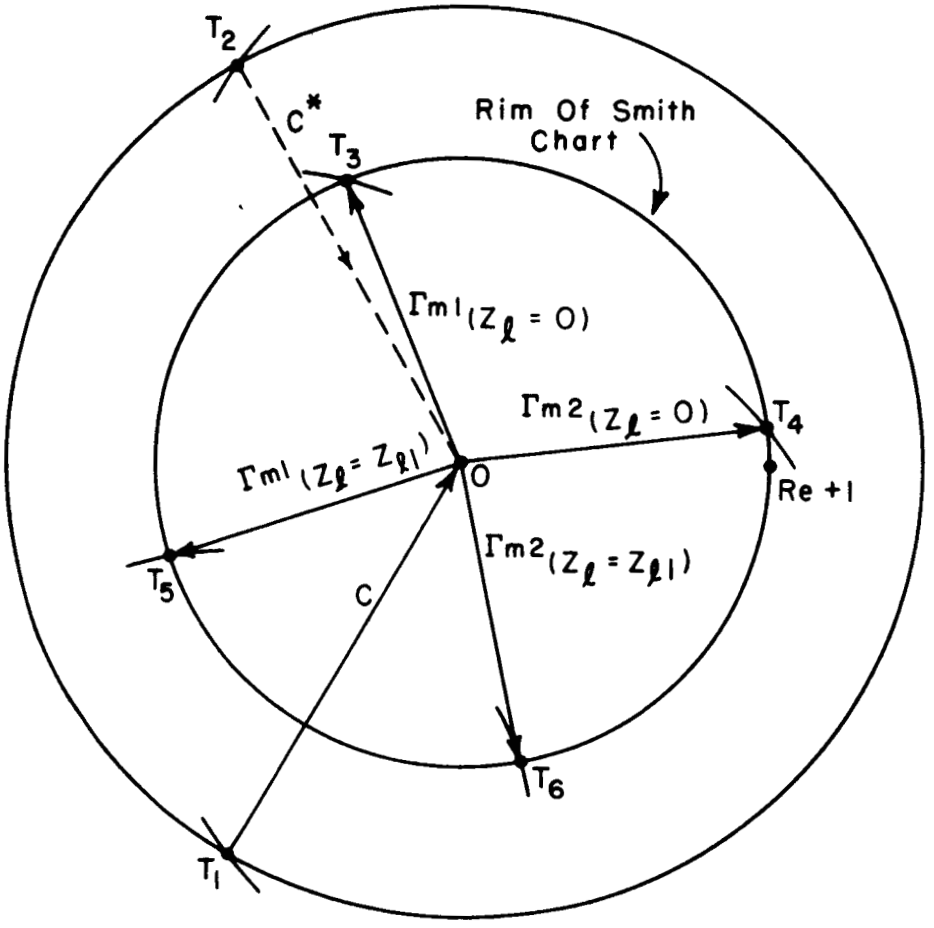

Fig. 14. Graphical solution for system nulled at no target (Case 4).

intersecting the circle, the radius of which is $|C|$ at points T_1 and T_2 (see Fig. 14). Then T_1O or T_2O is the phasor C. Taking T_1O to represent the phasor C, with T_1 as center, draw an arc with magnitude

$$(59) \qquad r_1 = \left|\Gamma_1/B\right|_{Z_\ell = 0} = \sqrt{\kappa_2}\,[\,|C| + 1]$$

intersecting the Smith Chart circumference at T_3 and T_4. $\Gamma_m]_{Z_\ell = 0}$ is either OT_3 or OT_4. With T_1 as center draw an arc with magnitude

$$(60) \qquad r_2 = \left|\Gamma_1/B\right|_{Z_\ell = Z_{\ell_1}} = \sqrt{\kappa_1}\,(\,|C| + 1)$$

intersecting the rim of the Smith Chart at T_5 and T_6. $\Gamma_m]_{Z_\ell = Z_{\ell_1}}$ is either OT_5 or OT_6.

The antenna impedance can be obtained by solving Eq. (42) where $\Gamma_m]_{Z_\ell = Z_{\ell_1}}$ and $\Gamma_m]_{Z_\ell = 0}$ are extracted from Fig. 14. It is apparent that if T_2O is taken as C, there would result a complex set of $\Gamma_m]_{Z_\ell = Z_{\ell_1}}$ and $\Gamma_m]_{Z_\ell = 0}$ found using T_1O as the phasor C. For the same reasoning explained in Case 3 (see Eq. (45) and (46)) one set would result in a negative R_a/Z_{c_2}, which is not the case for a passive antenna. The correct value of R_a/Z_{c_2} and X_a/Z_{c_2} could be selected from the many possibilities when using the information from Case 1, 2, or 3 or selecting the Z_a whose calculated echo-area-versus-load curve would agree with the experimentally measured one.

Figures 12, 13, and 14 were constructed from the data extracted from the calculated curves of Fig. 11, where $C = 1.5\angle 60°$ and $Z_a^*/Z_{c_2} = 1.2 - j0.8$. Then from the data extracted from Figs. 12 and 13 we find that $R_a/X_a = \pm 1.5$ and $Z_a^*/Z_{c_2} = 1.2 - j0.8$. The vector C ($T_1O$, Fig. 14) is seen to be $1.5\angle 60°$. The results agree with the original preselected values. The gain of the antenna and the prediction of the echo area for any load are found by the methods presented in Appendix B.

CHAPTER V
EXPERIMENTAL RESULTS

The different methods of measuring antenna parameters are now compared and the graphical method of estimating the distribution in Z_a^*/Z_{c_2} caused by recording and load errors is compared to an experimentally measured distribution.

Results from the programmed load method and the non-programmed load method for both the graphical solution and the mathematical solution are presented making use of experimental data appearing in Reference 4.

A. Programmed Load Method

The results of several gain and impedance measurements at 10.00 Kmc of the antennas shown in Fig. 16 measured by the slotted line method, gain comparison method, and scattering technique are presented in Table II and Fig. 16. It can be observed that there is good agreement between the standard methods and the scattering method.

To illustrate the method of estimating error in the input impedance by the scattering method, use is made of the appropriate graphs of Figs. 2-8. The results of the antenna designated C in Fig. 15 for the case where the echo area is forced to zero are

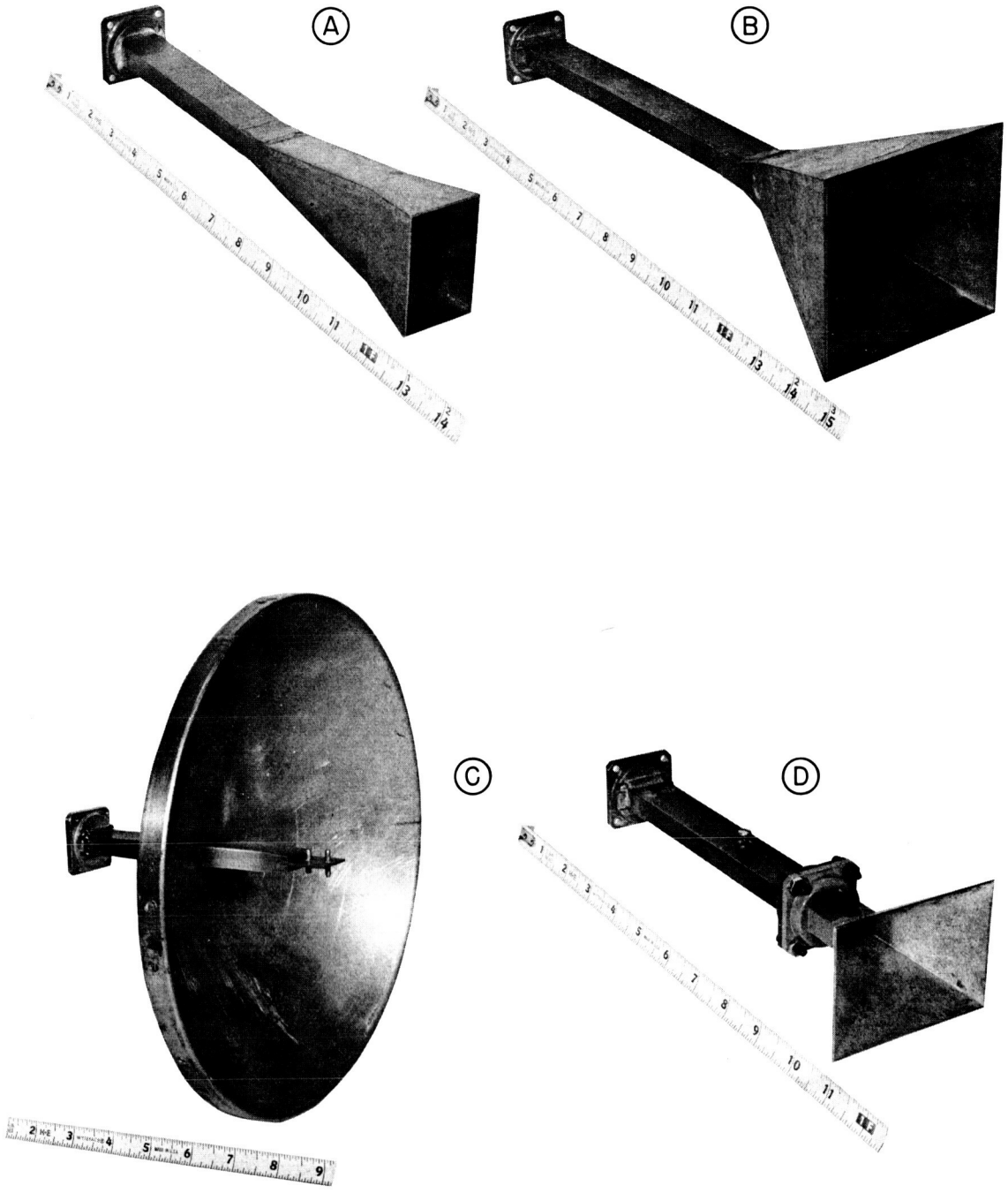

Fig. 15. Photograph of antennas (designated A, B, C, and D).

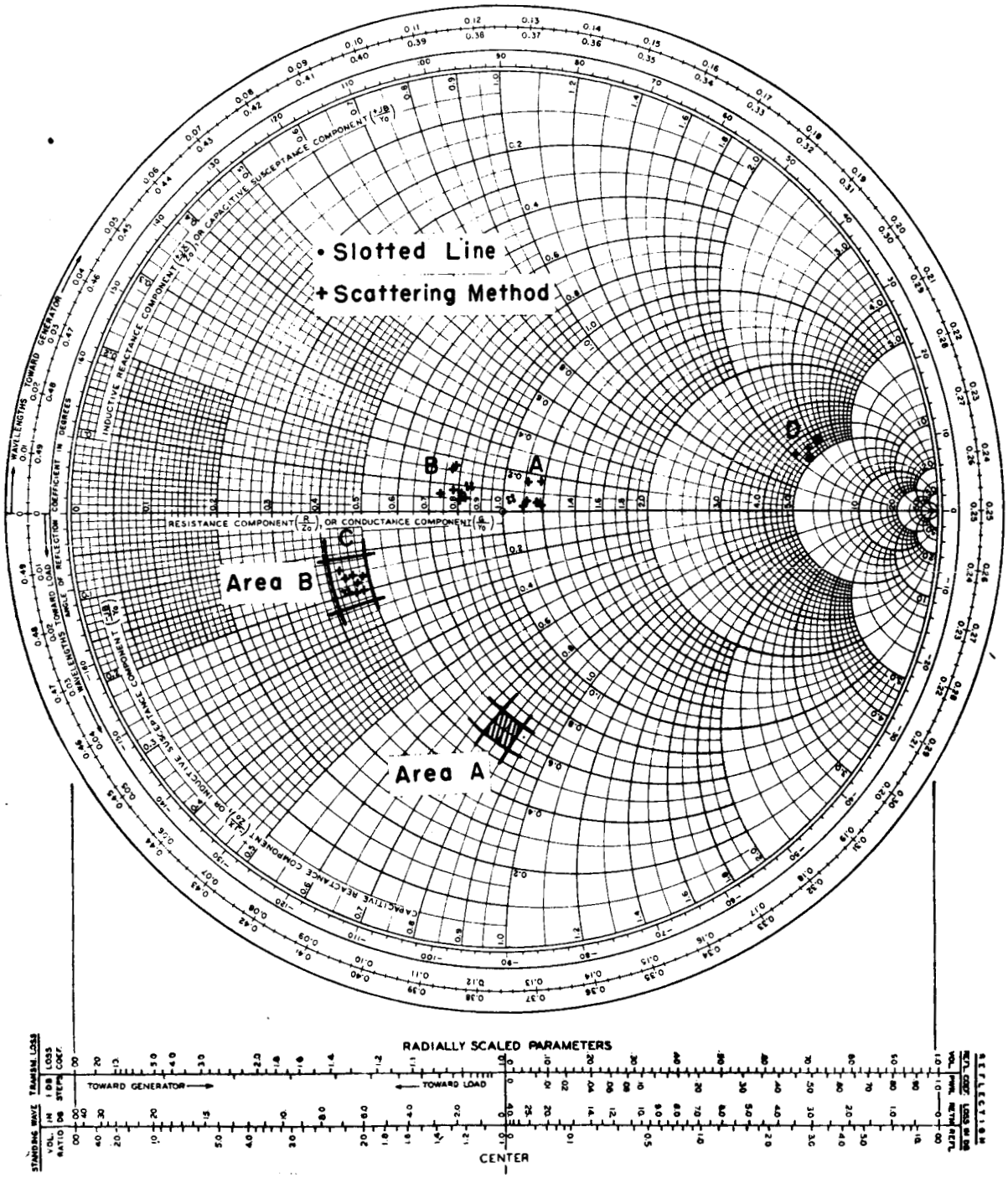

Fig. 16. Comparison of antenna impedance values obtained by slotted line and scattering method at 10.00 Kmc. Area A, typical illustration of estimating distribution of Z_a/Z_{c_2} by graphical analysis. Area B, estimated error of antenna designated C in text.

presented. The experimentally measured echo-area-versus-load characteristics using the programmed load are presented in Fig. 17, from which the loads causing minimum and average cross section are extracted. The load values are plotted on the Smith Chart and the complex conjugate of the antenna input impedance is found using geometrical constructions (see Fig. 18).

TABLE II
Comparison of Gain Values of the Antennas
Shown in Fig. 15 at 10.00 Kmc

Antenna	A	B	C	D
Ideal $\frac{4\pi A}{\lambda^2}$	13.9 db	20.4 db	29.2 db	18.1 db
Standard Method	14.1 db	18.4 db	27.2 db	14.9 db
Scattering Method	14.4 db	18.3 db	26.2 db	15.5 db

The gain of antenna C is found using the calibrated maximum echo area value extracted from Fig. 17 in Eq. (66) ($\sigma_{min} = 0$) and found to be 27.2 db.

With a load error estimated at $\pm 0.0025\lambda_g$ and recording error (relative error of ± 0.25 db) of $\pm 0.002\ \lambda_g$ in $X_\ell^{avg\ 1}$, $\pm 0.0015\lambda_g$ in $X_\ell^{avg\ 2}$, and zero in X_ℓ^{min} (this is practical since X_ℓ^{min} is at a null), the possible values of Z_a/Z_{c_z} and Z_a^*/Z_{c_z} are determined and represented graphically in Figs. 16 and 18, areas B and A, respectively. The combined total errors in the loads are shown in Fig. 18. The range of R_a is found using Fig. 7 (see shaded area), and the range of

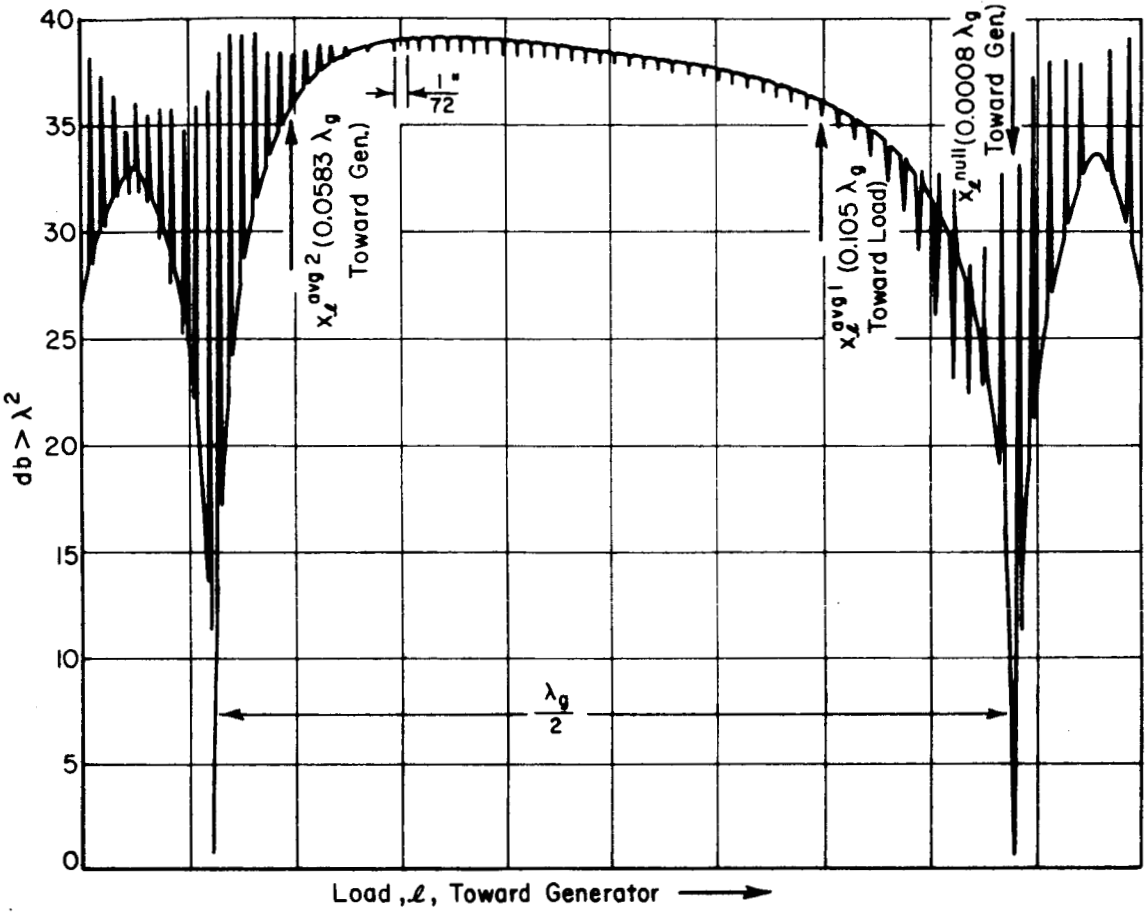

Fig. 17. Experimental echo-area-versus-load (programmed) patterns of antenna C (σ_{min} forced to zero).

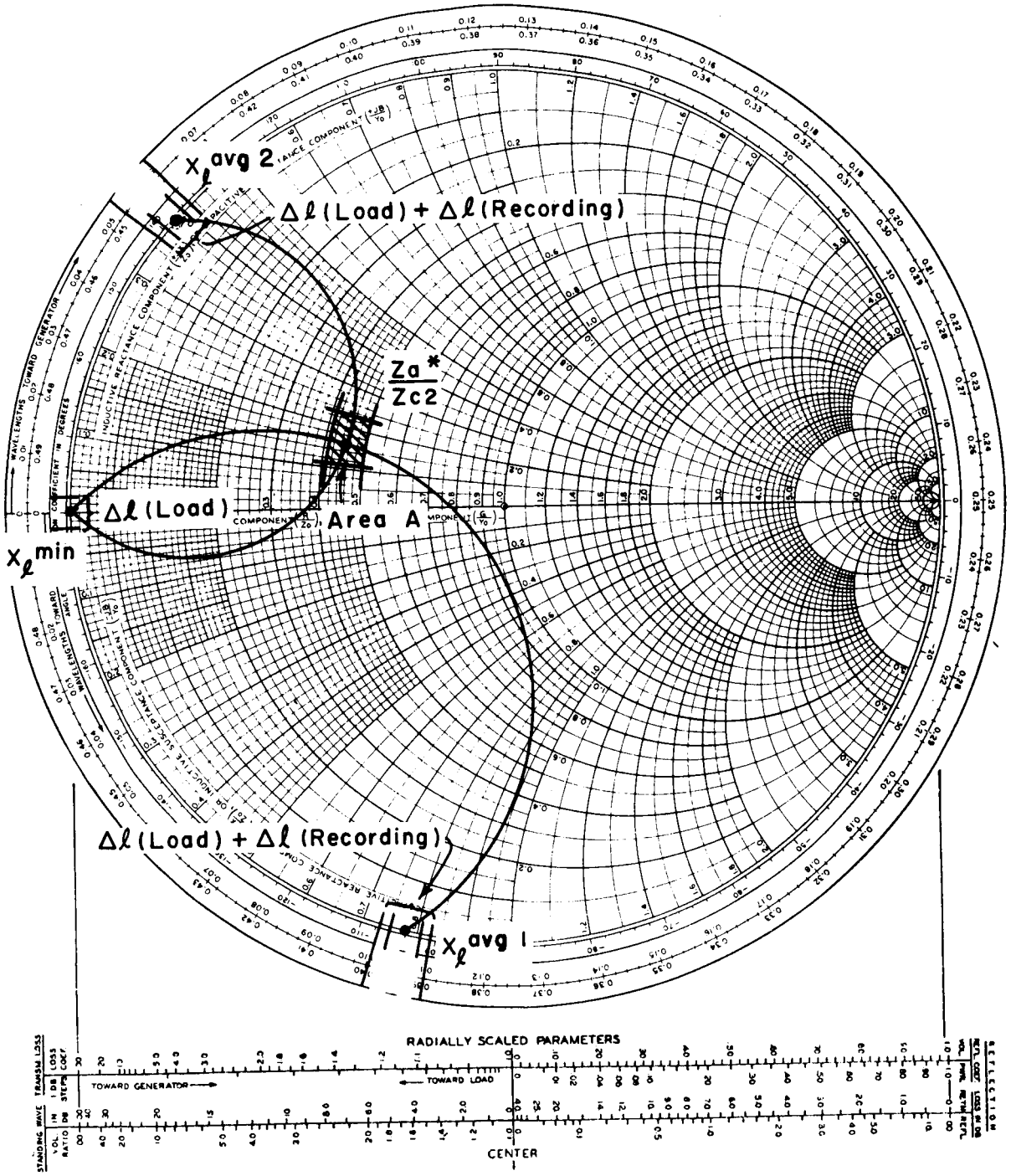

Fig. 18. Graphical determination of Za^*/Z_{c_2} and error analysis of antenna C for $\pm$ 0.0025λ load inherent error and recorder error of $\pm$ 0.002λ in X_ℓ^{avg1} and $\pm$ 0.0015λ in X_ℓ^{avg2}.

$X_a + X_\ell^{\text{avg 1}}$ is found using Fig. 8 (see area B). Since the range of $X_\ell^{\text{avg 1}}$ is known, the range of X_a is found. The estimated range of Z_a/Z_{c_2} is reasonable when compared to the range of the several measured values taken by the scattering technique.

B. Non-programmed Load Method

The experimentally measured echo-area-versus-load characteristics in Fig. 19 also appear in Reference 4 and are representative of Case 3. Using the programmed load technique reviewed in Appendix B we obtain $\frac{Z_a}{Z_{c_2}} = 0.96 + j0.21$ (see Fig. 20).

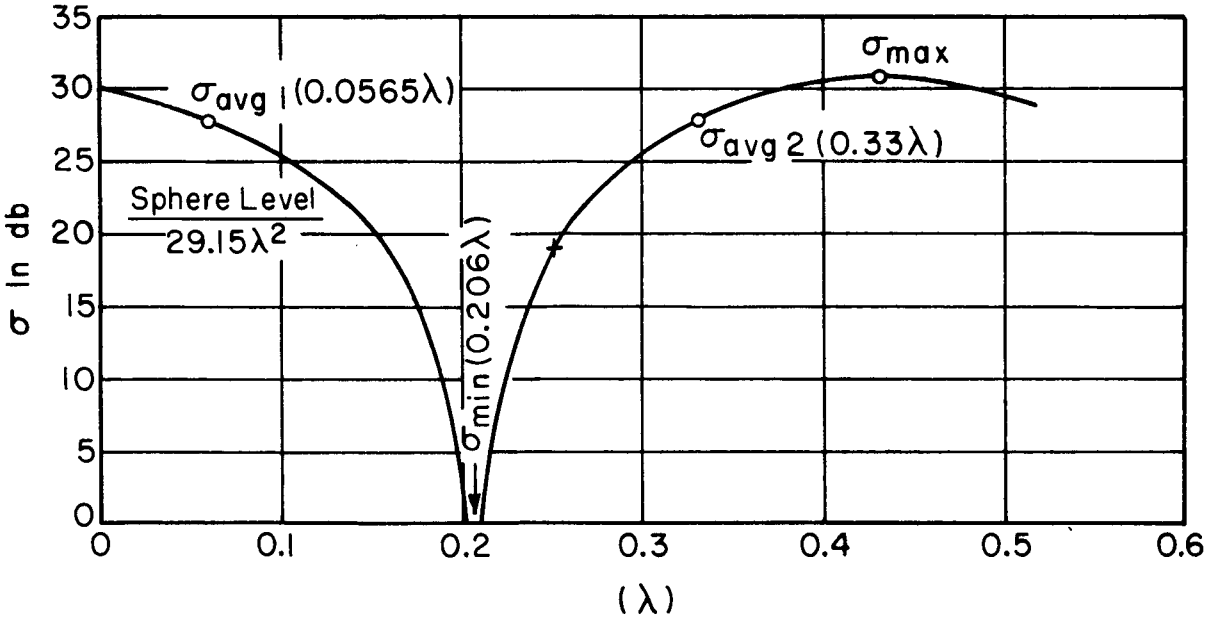

Fig. 19. Experimental echo-area-versus-load (in wavelengths toward the generator).

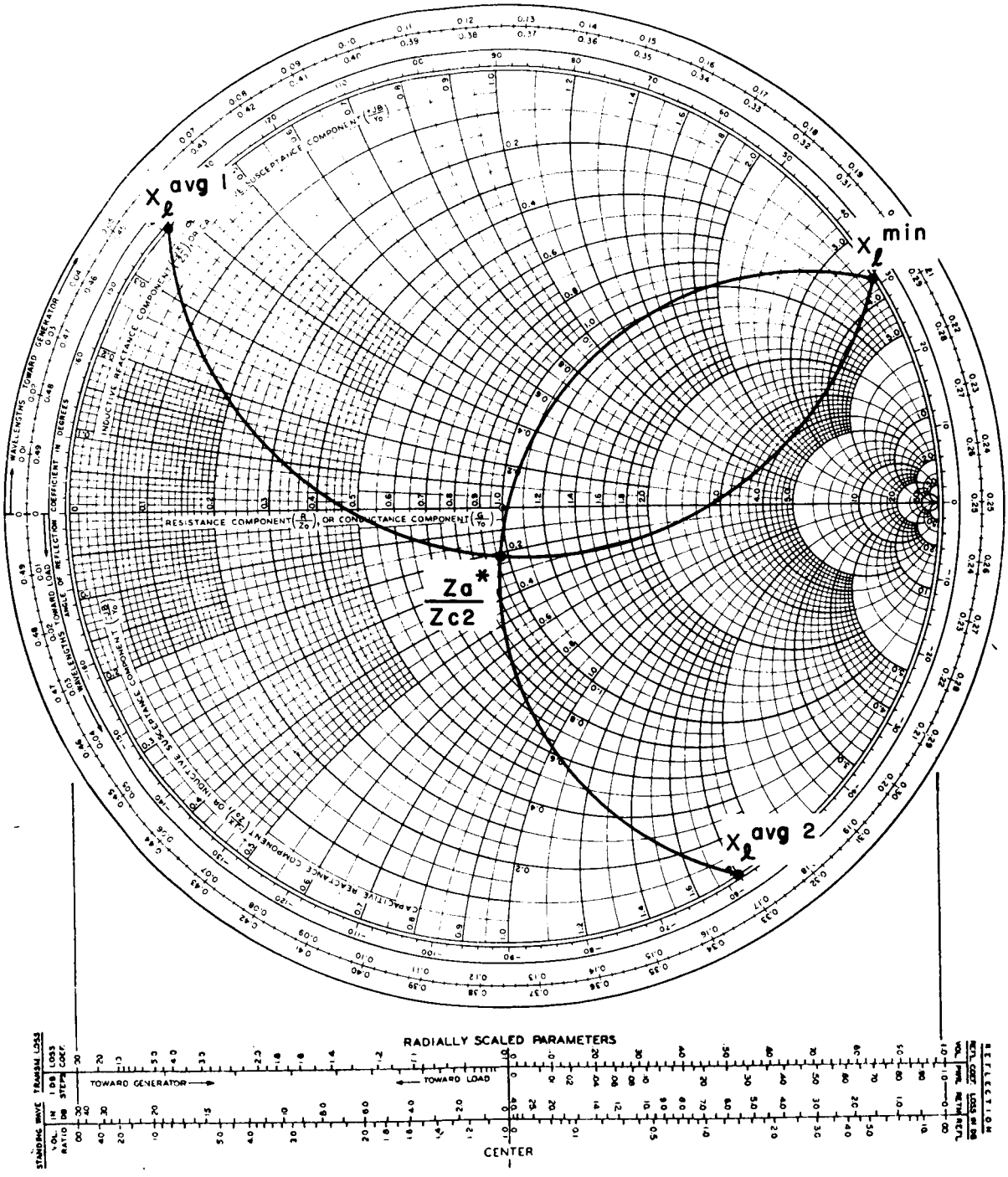

Fig. 20. Determination of Z_a^* / Z_{c_2} from data extracted from the curve of Fig. 19 by the method outlined in Appendix B.

For the non-programmed load technique, the following data are extracted from Fig. 19:

σ_{max} 31 $\Rightarrow$ -0 db 18.20 cm = $|\Gamma_1/B|^{max}$ (diameter of Smith Chart),

$\sigma]_{Z_\ell=\infty}$ 19 $\Rightarrow$ -12 db 4.57 cm = $|\Gamma_1/B|_{Z_\ell=\infty}$, and

$\sigma]_{Z_\ell=0}$ 30 $\Rightarrow$ -1 db 16.22 cm = $|\Gamma_1/B|_{Z_\ell=0}$.

Using the graphical method of Chapter III, Case 3, we find that (see Fig. 21)

$$\Gamma_m]_{Z_\ell=0} = 1\angle 155.5^\circ \text{ or } 1\angle -97.2^\circ; \quad \Gamma_m^*]_{Z_\ell=0} = 1\angle -155.5^\circ \text{ or } 1\angle +92.2^\circ$$

$$C = -\angle 29^\circ \quad , \quad C^* = -1\angle -29^\circ.$$

$Z_{\ell_1} = 0.206\lambda$ towards the generator.

From Eq. (43), we find that

$$\frac{Z_a}{Z_{c_2}} = 0.970 + j0.211 \text{ or } \frac{Z_a}{Z_{c_2}} = 0.745 - j0.657 \text{ and}$$
$$\frac{Z_a}{Z_{c_2}} = -0.970 + j0.211 \text{ or } \frac{Z_a}{Z_{c_2}} = -0.745 - j0.657.$$

Since R_a is positive for a passive antenna,

$$\frac{Z_a}{Z_{c_2}} = 0.970 + j0.211 \text{ or } \frac{Z_a}{Z_{c_2}} = 0.745 - j0.657.$$

A quick graphical check will show that σ_{max} would occur at 0.019λ towards the generator when using $\frac{Z_a}{Z_{c_2}} = 0.745 - j0.657$ and 0.447λ towards the generator when using $\frac{Z_a}{Z_{c_2}} = 0.970 + j0.211$. Therefore $\frac{Z_a}{Z_{c_2}} = 0.970 + j0.211$ is the correct antenna impedance.

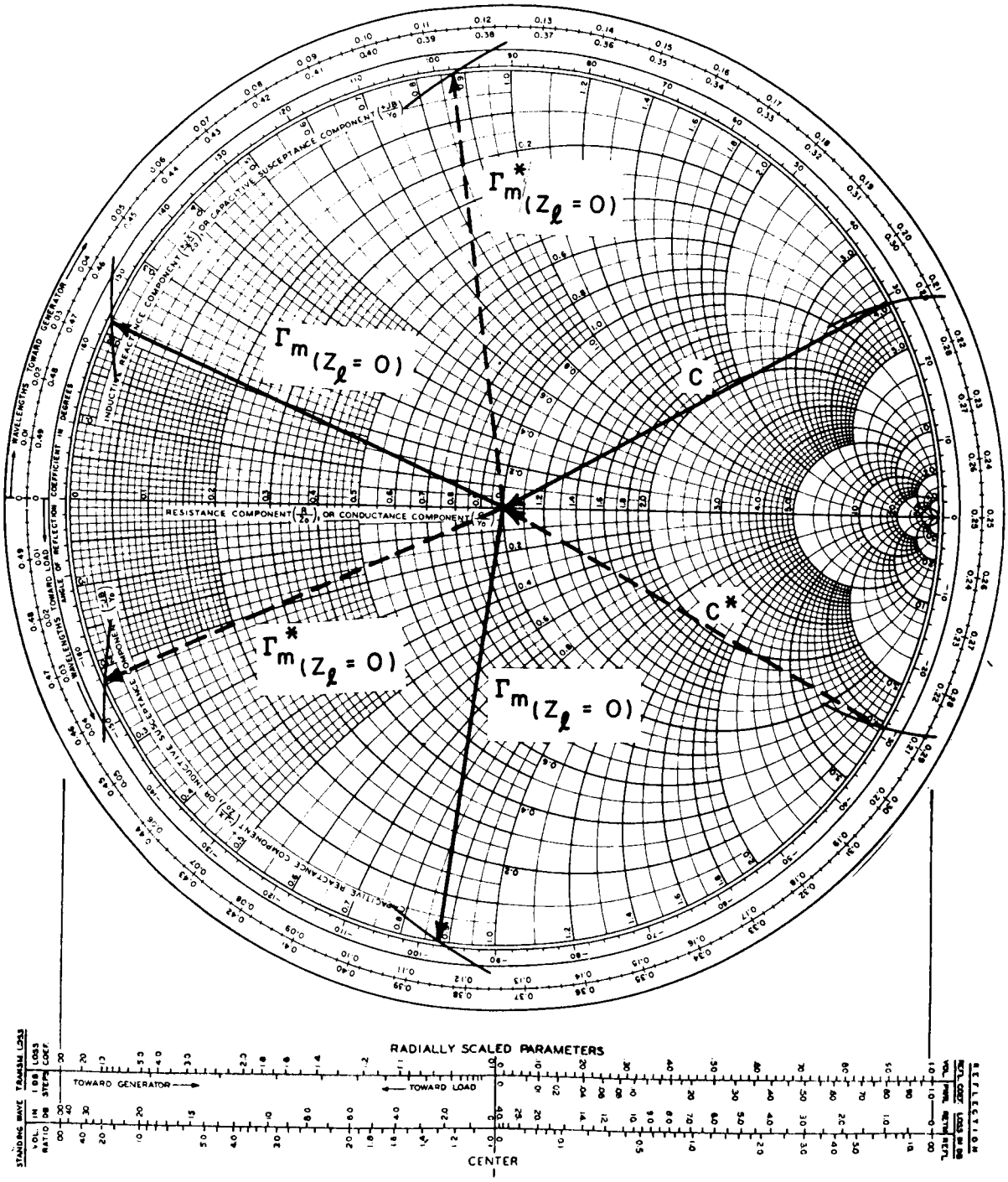

Fig. 21. Graphical solution of Z_a^*/Z_{c2} from data extracted from curve of Fig. 19 by the alternate method of Section IV.

Also G_3 and G_4 appearing in Eqs. (40) and (41) are $G_3 = -12$ db $= 0.0631$, and $G_4 = -1$ db $= 0.7943$, which are the values taken from Fig. 19. Using Eqs. (40) and (41) leads to essentially the same results.

CHAPTER VI
DISCUSSION

A description of a scattering method of measuring antenna parameters has been presented along with an error analysis. Experimental results for this method have been compared with results of conventional methods of measuring gain and impedance.

Gain measurements of three types of horn antennas and a dipole-fed dish determined by the standard gain method and the scattering method were found to be within a db and were nearly identical for two of the horn antennas. The variations in the measured gain values are attributed principally to the recording and calibration errors of each system.

Repeated measurements of input impedances of four antennas determined by the scattering technique were found to be distributed more than those obtained by the slotted line method. The reader is referred to Fig. 16 for a comparison of the distribution of the measured values of input impedance obtained by both methods. The greater distribution in the scattering method is attributed to the error in recording and in correlating the load with its respective echo area.

To relate the distribution in antenna input impedance resulting from errors in the recording and correlating systems, a graphical approach was presented because of the complicated fashion in which

the antenna impedance is related to the loads that cause maximum, minimum, and average echo area. The antenna input impedance can be determined via graphical constructions once these loads are known. For the dipole-fed antenna, designated C in the report, the estimated distribution in the possible values of the antenna input impedance due to a load correlation error of $\pm 0.0025\lambda_g$ and a relative recording error of ± 0.25 db was found to be in close agreement with the measured distribution.

There are many types of antennas that may have nearly the same input impedance but with different structural scattering characteristics. There are several combinations of three loads out of a possible four that may yield the same value of antenna input impedance. Because of the many variables and the complicated fashion in which they are related, the selection of the best possible combination to obtain a minimum distribution in the input impedance is not readily apparent.

To obtain a distribution in $\frac{Z_a}{Z_{c_2}}$ similar to that obtained using the slotted line method would require that the loads that cause maximum, minimum, and average echo area be known within about $0.001\lambda_g$ in the programmed load used in this report. This should not distract from the usefulness of the scattering method since there undoubtedly are many situations in which the results may be more accurate than slotted line measurements, even with $\pm 0.0025\lambda_g$ error in the programmed load.

An alternate approach to the scattering method using a non-programmed load has been presented in Section IV. In this method the load requirements are simpler and offer the possibility of significantly reducing load-positioning error. The results are obtained by using a particular set of loads rather than a programmed load, hence enabling accurate presetting of the loads and eliminating the correlation of the load with the respective point on the echo-area-versus-load characteristics. Furthermore, the direction in which greater accuracy results is more apparent if one assumes no load error. For example, in the graphical approach one procedure is to draw the arc having a center at +1 and equal to $|\Gamma_1/B|_{Z_\ell=\infty}$, and intersecting the rim of the Smith Chart. By controlling the fixed scattering component, the intersection can be made to fall other than near 0λ toward the generator or load on the Smith Chart where a slight error in $|\Gamma_1/B|_{Z_\ell=\infty}$ will have its greatest effect.

The simpler non-programmed load requirements are gained at the expense of a more complicated procedure for determining the antenna input impedance. The method of determining gain is the same for both methods and the method of determining the phasor C by the non-programmed load method is not more complicated than the programmed load method although the procedure is different.

The scattering method of determining antenna parameters requires the use of a more complex measuring system and a more sophisticated mathematical or graphical approach than the standard methods. However, the scattering method may offer the best and possibly the only practical approach in some situations. For example, consider measuring the input impedance of a stub on a sphere. The transmission line and entrance on the sphere connecting the stub antenna to the transmission line may result in erroneous measurements. Several other advantages and disadvantages of the different methods were discussed in the introduction.

In view of the results obtained by the scattering method, it is concluded that it is a practical method for measuring antenna gain and impedance as well as echo area.

APPENDIX A

REVIEW OF CONVENTIONAL METHODS OF MEASURING IMPEDANCE, GAIN, AND SCATTERING CROSS SECTIONS

The determination of impedance by the Slotted Line Method[6] makes use of the experimental set-up shown in the block diagram of Fig. 22(a), and a graphical solution employing a Smith Chart. With the unknown impedance connected to the terminals, the impedance at the probe position, where VSWR minimum occurs, is located on the Smith Chart using the measured value of VSWR $\left(\frac{E_{max}}{E_{min}}\right)$ and the fact that the normalized impedance is real and less than or equal to one at a voltage minimum. The impedance at the terminals is then found by a rotation toward the load on a constant VSWR circle of the distance in guide wavelengths from the position of the minimum to the position of the load. Usually the distance from the load terminals to a point on the slotted line is calibrated using a short at the load terminals.

The principal sources of error for the Slotted Line Method are frequency drift, phase shift at connections, probe distortion of slotted line fields, slot leakage, crystal nonlinearity, and the reading of the probe position. With calibrated curves the total error could be attributed to the slotted line itself. The best possible results would be related to the minimum measurable VSWR and to the

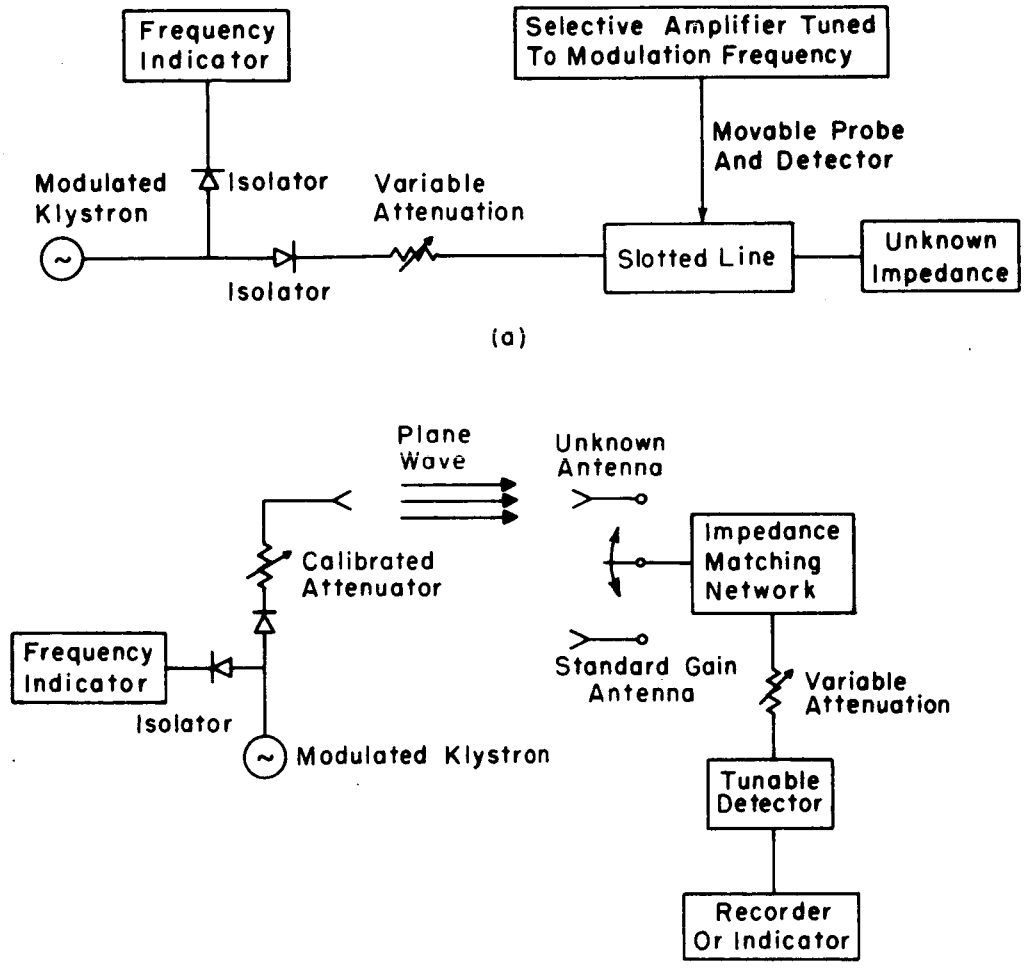

Fig. 22. Block diagram: (a) typical slotted line impedance measuring system, (b) typical gain comparison measuring system.

accuracy with which the probe location could be read. For the several VSWR measurements which were taken with reasonable care and cited in this report, the probe positions were within $0.001\lambda_g$ of the correct position and the VSWR within at least 2% on the Smith Chart. There are methods to correct for errors (see Reference 6) which constitute experiments in themselves since each system may be different and must be analyzed separately.

A block diagram of a typical antenna range for conventional gain measurements[6] is presented in Fig. 22(b). The performance of an unknown antenna is compared to that of a precalibrated standard gain antenna. The attenuator in the transmitter arm is adjusted to maintain constant input to the receiving system (this overcomes any nonlinearities in the system) and the difference in reading of the attenuator is added (or subtracted if the unknown antenna has less gain than the standard) to the precalibrated antenna value to obtain the gain of the unknown antenna. The accuracy of the attenuator and the precalibrated antenna determine the accuracy of the results.

A block diagram of a typical cw scattering range is shown in Fig. 23.[10] The energy scattered by a target is usually recorded on a strip chart in db as a function of target rotation or as a function of load variation at a fixed aspect. The accuracy of the overall system,

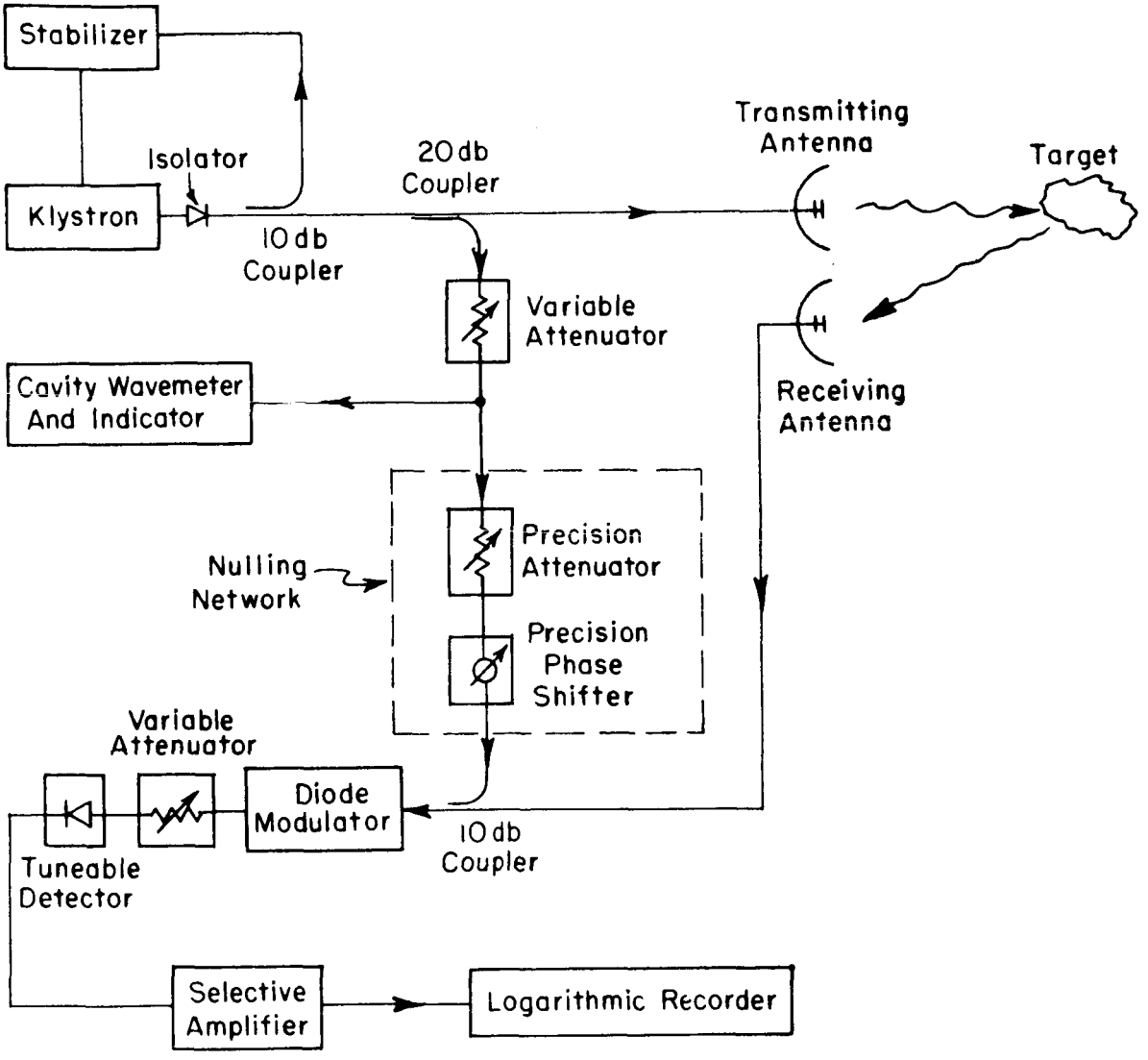

Fig. 23. Block diagram, typical radar cross section measuring system.

as well as of the calibration, can be determined by measuring the cross sections of targets (spheres, cylinders, flat plates, etc.) that can be calculated analytically.

A portion of the transmitted signal may be coupled back into the receiving system with controlled magnitude and phase to either cancel any unwanted signal or add to a scattered signal. In this way undesired background signal can be significantly reduced and will result in better system sensitivity.

APPENDIX B
THE DETERMINATION OF ANTENNA PARAMETERS BY SCATTERING CROSS SECTION MEASUREMENTS

The method of relating the gain, echo area, and impedance of an antenna to its scattering properties treats the antenna as a scatterer whose terminals are loaded with a variable reactive load. The antenna under investigation, the radar transmit-receiver antenna, and the intervening space are considered to be a linear, passive, reciprocal two-port network (Fig. 24), under the conditions

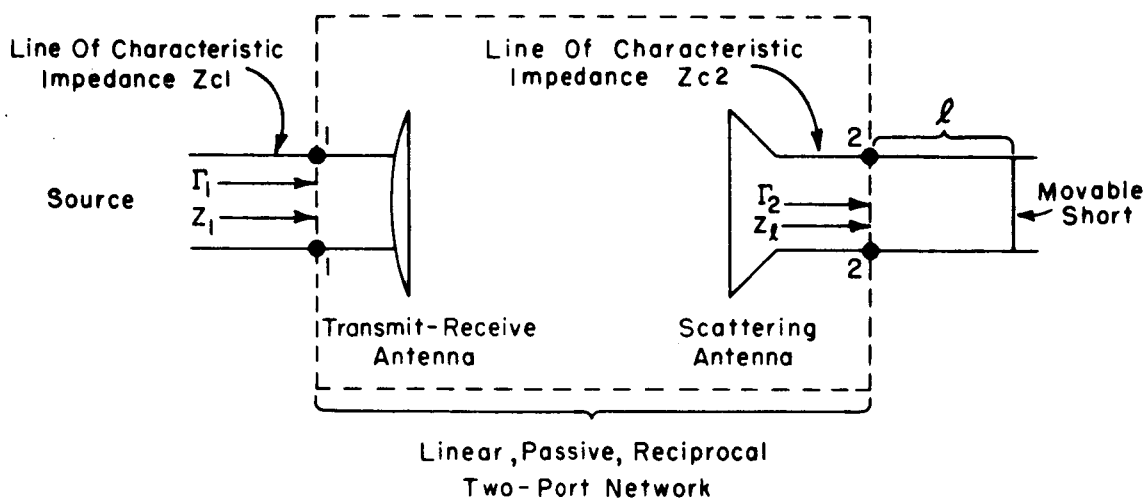

Fig. 24. Diagram of two-port network.

This appendix is a brief summary of References 1, 4, and 5. References 7, 8, and 9, keyed in the text, describe earlier work and are also referred to in References 1, 4, and 5.

that the coupling between the antennas is negligible. This is valid for a fixed antenna, polarization, and frequency. Terminals 1-1 and 2-2 in Fig. 24 represent the transmit-receive antenna terminals and the scattering antenna terminals, respectively. The voltage reflection coefficients are defined by

$$\Gamma_1 = \frac{Z_1 - Z_{c_1}}{Z_1 + Z_{c_1}} \tag{61}$$

at 1-1, and

$$\Gamma_2 = \frac{Z_\ell - Z_{c_2}}{Z_\ell + Z_{c_2}} \tag{62}$$

at terminals 2-2 (see Fig. 24 for definitions of Z_ℓ, Z_{c_1}, Z_{c_2}).

For a typical scattering system, the scattering cross section is defined by

$$\sigma = \kappa \left|\Gamma_1\right|^2, \tag{63}$$

where κ may be determined by employing a calibrated reference target.

For a linear, passive, reciprocal two-port network, a linear relationship of the form

$$\Gamma_1 = A + B\Gamma_m = B(C + \Gamma_m) \tag{64}$$

exists between the input reflection coefficient, Γ_1, and the

load-dependent, modified reflection coefficient Γ_m defined by

$$\Gamma_m = \frac{Z_\ell - Z_a^*}{Z_\ell + Z_a} \quad , \tag{65}$$

where Z_ℓ is the load impedance and Z_a the antenna impedance of the antenna under test. When Z_ℓ is purely reactive, $|\Gamma_m|$ will be equal to unity.

The form of Γ_m permits the use of a Smith Chart superimposed on a complex plane, (open-circuit point at +1), to graphically illustrate the load-dependence of the reflection coefficient, Γ_1 (Fig. 25).[7] With the constants C, B, or κ, and the load reflection coefficient, Γ_2, that give maximum, minimum, and average scattering cross sections for the case where Z_{c_2} is real and Z_ℓ purely reactive, the impedance, gain, and cross section for any load on the scattering antenna can be found. Since Z_ℓ is purely reactive, the points $\frac{jX_\ell}{Z_{c_2}}$ and Γ_2 are the same and will lie on the rim of the Smith Chart (assumed to have unit radius).

The complex conjugate of the input impedance of the scattering antenna is determined by the intersection of two circles (four possibilities), illustrated in Fig. 26. Points a and b are any two convenient points 90° apart on the rim of the Smith Chart. This is a result of the Γ_m (related to echo area maximum, average 1, minimum, and average 2) having 90° phase difference. By an inversion rotation process through an inversion point, $\frac{Z_a^*}{Z_{c_2}}$ (the

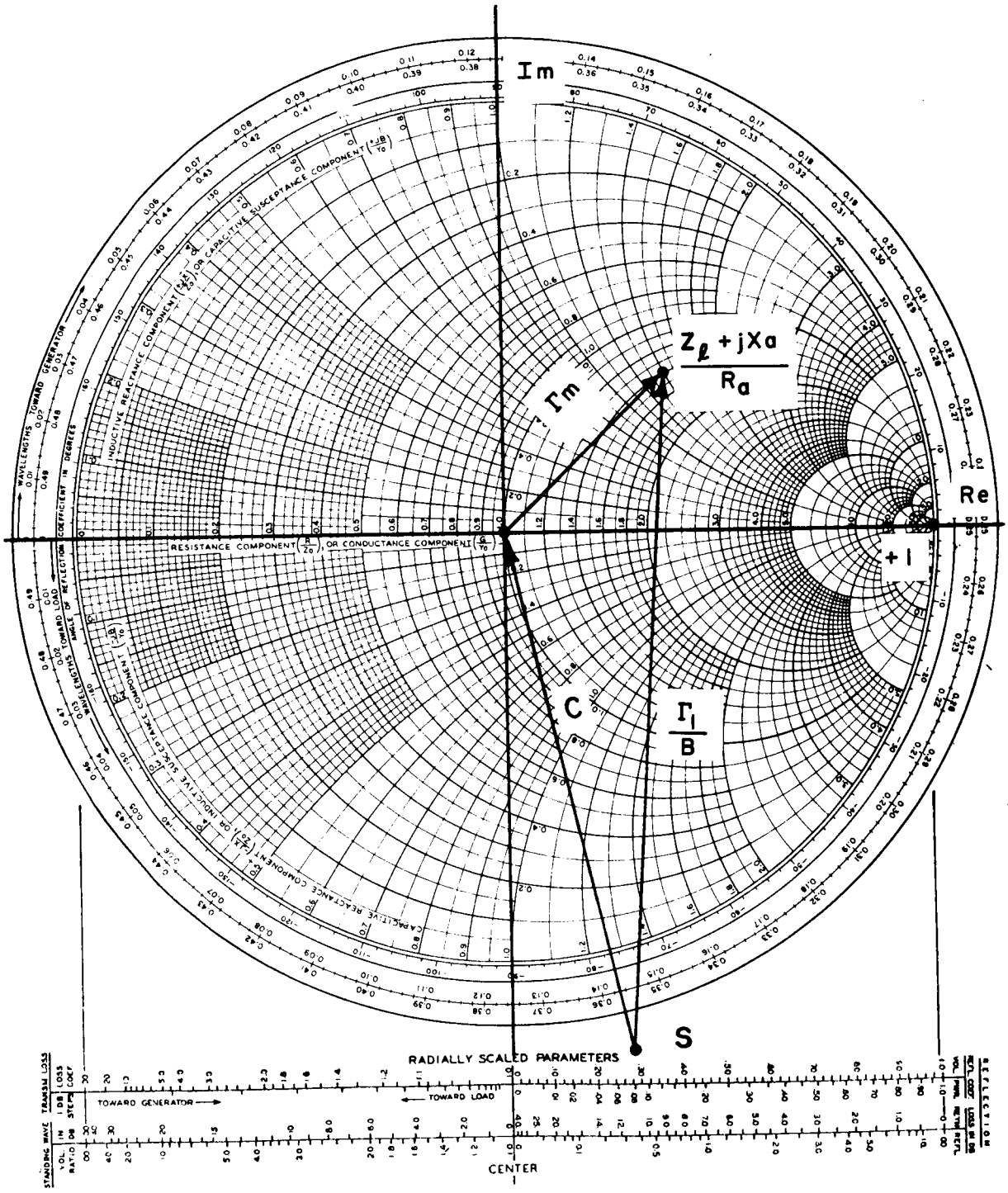

Fig. 25. Graphical representation of signal scattered by an antenna as a function of load.

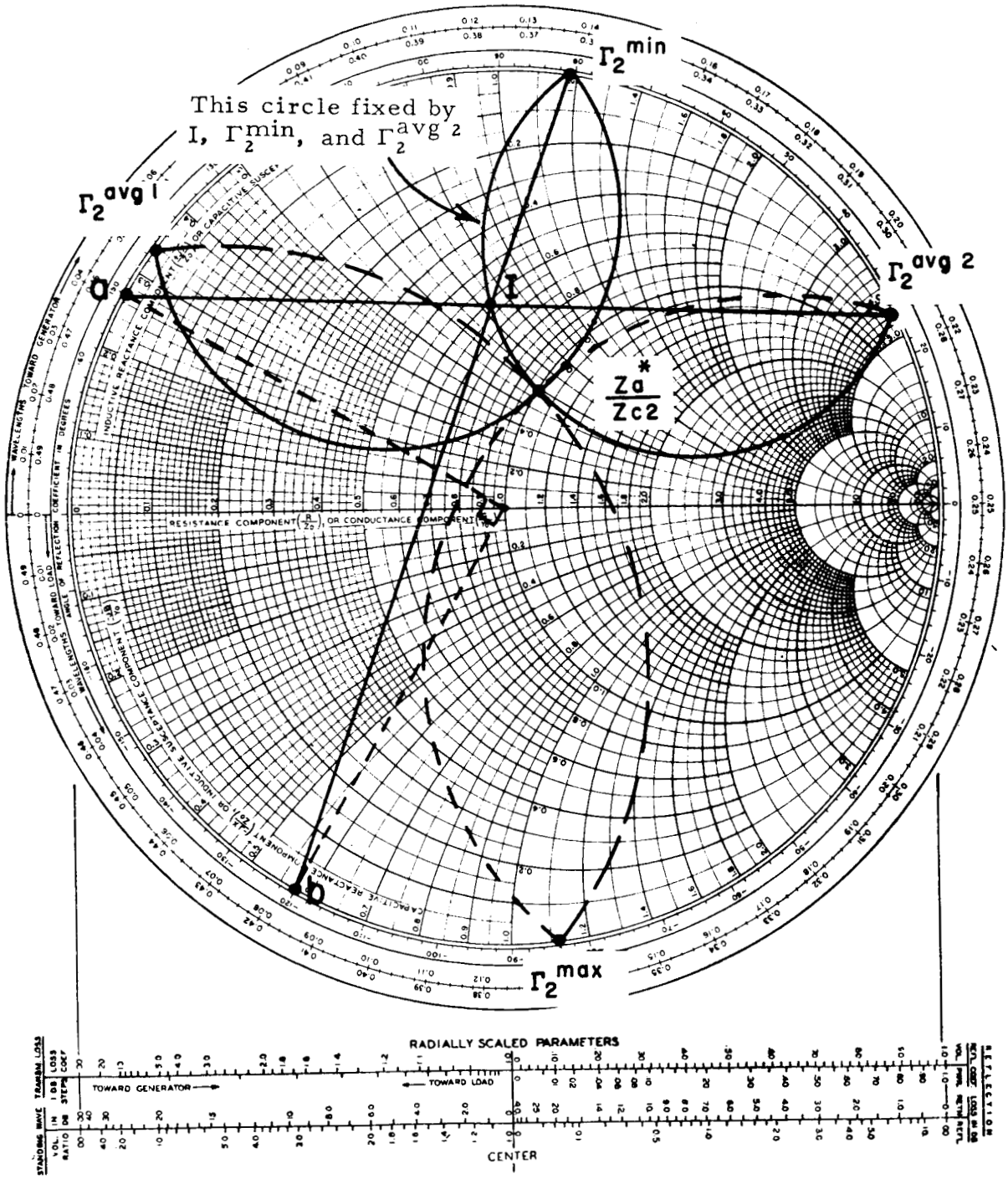

Fig. 26. Graphical determination of Z_a^*/Z_{c_2}.

normalized complex conjugate of the antenna impedance), the Γ_z and their respective Γ_m can be found (a typical illustration is shown in Fig. 27).

The gain is related to the scattering cross section by

$$G_r G_t = \frac{\pi}{p_r p_t} \frac{\left(\sqrt{\sigma_{max}} \pm \sqrt{\sigma_{min}}\right)^2}{\lambda^2} , \tag{66}$$

where G_r and G_t are the power gains of the scattering antenna in the direction of the transmitting and receiving antenna, respectively, and p_r and p_t are polarization mismatch factors.[8,9]

The ambiguity in Eq. (66) can be resolved by forcing σ_{min} to zero or by employing a lossy load. The magnitude of the phasor C is related to the scattering cross section by

$$|C| = \frac{\pi(\sigma_{max} - \sigma_{min})}{p_r p_t G_r G_t \lambda^2} , \tag{67}$$

and its phase is that of the phasor Γ_m^{max}. The echo area for any load can be found by the relationship

$$\sigma_{(Z_\ell)} = \left\{ \frac{|C + \Gamma_{m(Z_\ell)}|}{|C| + 1} \right\}^2 \sigma_{max} \tag{68}$$

or

$$\sigma_{(Z_\ell)} = \left\{ \frac{|C + \Gamma_{m(Z_\ell)}|}{|C| - 1} \right\}^2 \sigma_{min} ,$$

where σ_{max}, σ_{min}, the phasor C, and Z_a are the values obtained with

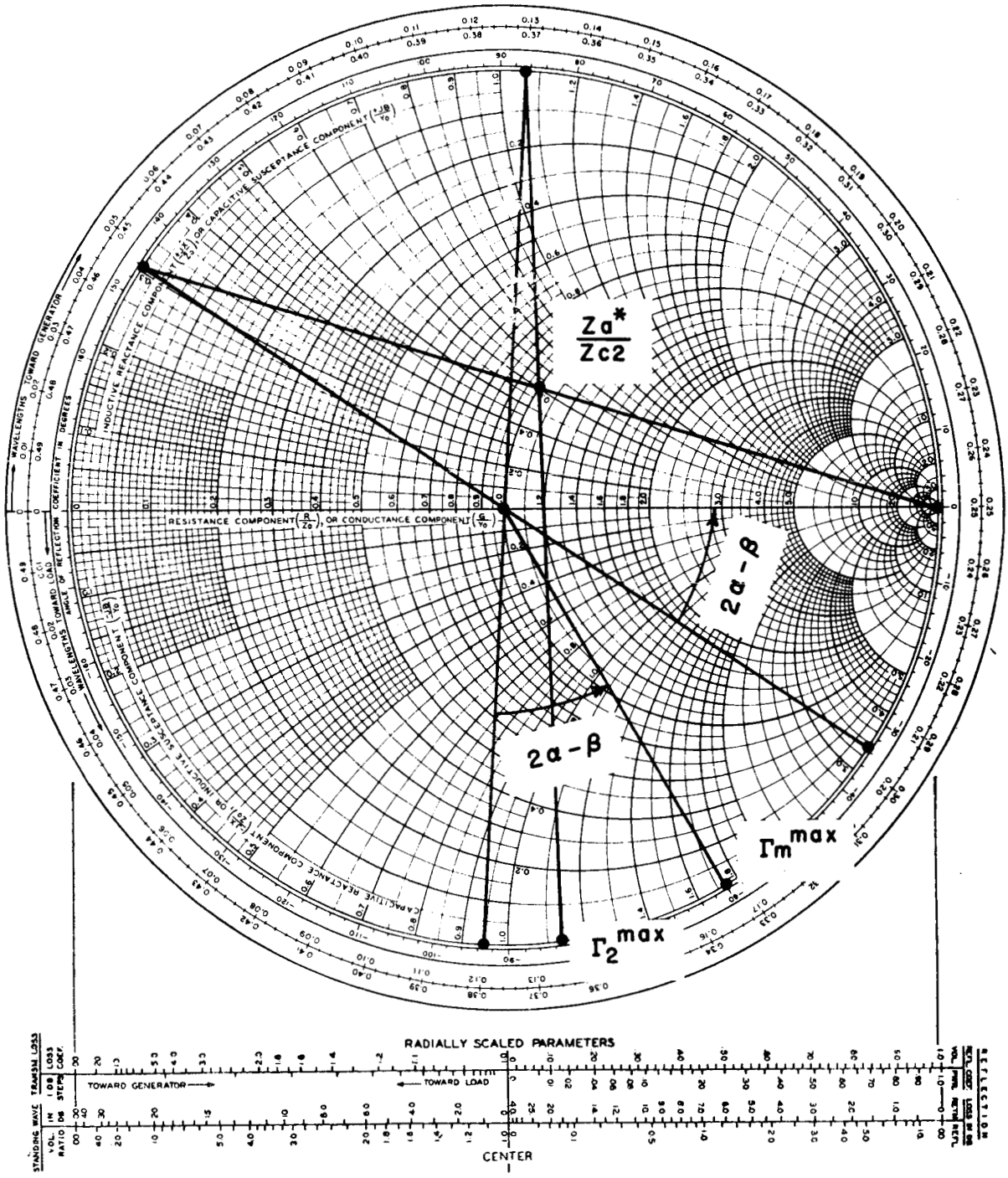

Fig. 27. Geometrical constructions relating Γ_2 and the respective Γ_m.

the use of a purely reactive load and the Smith Chart is assumed to have a unit radius. In Fig. 25 the phasor $\Gamma_m(Z_\ell)$ is found directly when the point $\frac{Z_\ell + jX_a}{R_a}$ is plotted on the Smith Chart.

APPENDIX C
THE RELATIONSHIP OF THE SLOPE, $\frac{d\sigma}{d\ell}$, TO THE MAGNITUDE AND PHASE RELATIONSHIP BETWEEN THE LOAD-DEPENDENT AND FIXED SCATTERING COMPONENT AND ANTENNA IMPEDANCE

The echo area normalized to σ_{max} is of the form

$$(69) \qquad \frac{\sigma}{\sigma_{max}} = \left| \frac{C + \Gamma_m}{C + \Gamma_m^{max}} \right|^2 ,$$

where C is a constant and Γ_m is a load dependent, modified, reflection coefficient (see Appendix B) of the form

$$(70) \qquad \Gamma_m = e^{j\phi} = \frac{jX_\ell - Z_a^*}{jX_\ell + Z_a} ,$$

when the load is purely reactive. The input impedance of a load consisting of a movable short in a transmission line is

$$(71) \qquad Z_\ell = jX_\ell = jZ_{c_2} \tan 2\pi\ell_\lambda ,$$

where ℓ_λ is the distance in guide wavelengths of the short to the load terminals and Z_{c_2} is the characteristic impedance of the transmission line.

Taking the derivative of Eq. (69) with respect to ℓ_λ,

$$(72) \qquad \frac{d(\sigma/\sigma_{max})}{d\ell_\lambda} = \frac{2|C|}{[|C| + 1]^2} \sin(\alpha - \phi) \frac{d\phi}{d\ell_\lambda} ,$$

where $C = |C| e^{j\alpha}$.

Solving for $\sin\phi$ and $\cos\phi$ in Eq. (70),

$$\sin\phi = \frac{2R_a(X_\ell + X_a)}{R_a^2 + (X_\ell + X_a)^2} \tag{73}$$

and

$$\cos\phi = \frac{-R_a^2 + (X_\ell + X_a)^2}{R_a^2 + (X_\ell + X_a)^2} \tag{74}$$

Taking the derivative of Eq. (73) with respect to ℓ_λ and making use of Eq. (74),

$$\frac{d\phi}{d\ell_\lambda} = \frac{1 - \cos\phi}{R_a/Z_{c_2}} \quad \frac{dX_\ell/Z_{c_2}}{d\ell_\lambda} \tag{75}$$

By substituting Eq. (75) into Eq. (72),

$$\frac{d(\sigma/\sigma_{max})}{d\ell_\lambda} = \frac{2|C|\sin(\alpha-\phi)(\cos\phi - 1)}{[|C| + 1]^2 R_a/Z_{c_2}} \quad \frac{d(X_\ell/Z_{c_2})}{d\ell_\lambda} , \tag{76}$$

which leads to

$$\frac{d(\sigma/\sigma_{max})}{d\ell_\lambda} = \frac{2|C|\sin(\alpha-\phi)(\cos\phi-1)}{[|C| + 1]^2 R_a/Z_{c_2}} \; 2\pi\sec^2 2\pi\,\ell_\lambda , \tag{77}$$

where, from Eq. (71),

$$\frac{d(X_\ell/Z_{c_2})}{d\ell_\lambda} = 2\pi\sec^2 2\pi\,\ell_\lambda .$$

APPENDIX D
THE RELATIONSHIP BETWEEN ANTENNA IMPEDANCE AND THE LOADS THAT CAUSE σ_{max}, σ_{min}, $\sigma_{avg\ 1}$, and $\sigma_{avg\ 2}$

Because of the 90° phase relationship between Γ_m^{max}, Γ_m^{min}, $\Gamma_m^{avg\ 1}$, and $\Gamma_m^{avg\ 2}$, we can form the following relationships:

$$\Gamma_m^{avg\ 2} \cdot \Gamma_m^{*\ avg\ 1} = -1 \tag{78}$$

$$\Gamma_m^{max} \cdot \Gamma_m^{*\ min} = -1 \tag{79}$$

$$\Gamma_m^{max} \cdot \Gamma_m^{*\ avg\ 1} = j \tag{80}$$

$$\Gamma_m^{avg\ 1} \cdot \Gamma_m^{*\ min} = j \tag{81}$$

$$\Gamma_m^{avg\ 2} \cdot \Gamma_m^{*\ max} = j \tag{82}$$

$$\Gamma_m^{min} \cdot \Gamma_m^{*\ avg\ 2} = j\,. \tag{83}$$

The solutions of R_a and X_a in terms of any three loads consist of the same procedure regardless of what three loads are selected. The development of R_a and X_a as functions of $X_\ell^{avg\ 1}$, $X_\ell^{avg\ 2}$, and X_ℓ^{min} is presented and the results of the remaining three possibilities are stated in Table 1, Chapter II, of this report.

By expanding the equations containing $X_\ell^{avg\ 1}$, $X_\ell^{avg\ 2}$, and X_ℓ^{min} ((78), (81), and (83), using the definition of Γ_m (Eq. (65), and assigning the appropriate values of X_ℓ, we get

$$R_a^2 + X_a^2 = -X_\ell^{\text{avg 2}} X_\ell^{\text{avg 1}} - X_a(X_\ell^{\text{avg 2}} + X_\ell^{\text{avg 1}}), \tag{84}$$

$$R_a^2 + X_a^2 = -X_\ell^{\min} X_\ell^{\text{avg 1}} - X_a(X_\ell^{\text{avg 1}} + X_\ell^{\min}) - R_a(X_\ell^{\text{avg 1}} - X_\ell^{\min}), \tag{85}$$

and

$$R_a^2 + X_a^2 = -X_\ell^{\min} X_\ell^{\text{avg 2}} - X_a(X_\ell^{\min} + X_\ell^{\text{avg 2}}) - R_a(X_\ell^{\min} - X_\ell^{\text{avg 2}}) . \tag{86}$$

For example, Eq. (78) leads to

$$\frac{-R_a + j(X_\ell^{\text{avg 2}} + X_a)}{R_a + j(X_\ell^{\text{avg 2}} + X_a)} \cdot \frac{-R_a - j(X_\ell^{\text{avg 1}} + X_a)}{R_a - j(X_\ell^{\text{avg 1}} + X_a)} = -1, \tag{87}$$

which leads to Eq. (84). Subtracting Eq. (84) from Eq. (85) and (86),

$$R_a(X_\ell^{\min} - X_\ell^{\text{avg 2}}) + X_a(X_\ell^{\min} - X_\ell^{\text{avg 1}}) + X_\ell^{\text{avg 2}}(X_\ell^{\min} - X_\ell^{\text{avg 1}}) = 0 \tag{88}$$

and

$$R_a(X_\ell^{\text{avg 1}} - X_\ell^{\min}) + X_a(X_\ell^{\min} - X_\ell^{\text{avg 2}}) + X_\ell^{\text{avg 1}}(X_\ell^{\min} - X_\ell^{\text{avg 2}}) = 0. \tag{89}$$

Solving for R_a and X_a in Eqs. (88) and (89),

$$R_a = \frac{BH}{1 + H^2} \tag{90}$$

and

$$X_a = -c - R_a/H = -b + R_a H, \tag{91}$$

where

$$H = \frac{X_\ell^{\min} - X_\ell^{\text{avg } 1}}{X_\ell^{\min} - X_\ell^{\text{avg } 2}}, \quad B = X_\ell^{\text{avg } 1} - X_\ell^{\text{avg } 2},$$

$$b = X_\ell^{\text{avg } 1}, \text{ and } c = X_\ell^{\text{avg } 2}.$$

REFERENCES

1. Garbacz, R. J., "The Determination of Antenna Parameters by Scattering Cross-Section Measurements: I. Antenna Impedance," Report 1223-8, 30 September 1962, Antenna Laboratory, The Ohio State University Research Foundation; prepared under Contract AF 33(616)-8039, Aeronautical Systems Division, Air Force Systems Command, United States Air Force, Wright-Patterson Air Force Base, Ohio. AD 286 760

2. Kraus, J. D., Antennas, McGraw-Hill Book Company, Inc., New York, 1950.

3. Moffatt, D. L., "Determination of Antenna Scattering Properties from Model Measurements," Report 1223-12, 1 January 1964, Antenna Laboratory, The Ohio State University Research Foundation; prepared under Contract AF 33(616)-8039, Research Technology Division, Air Force Avionics Laboratory, Air Force Systems Command, United States Air Force, Wright-Patterson Air Force Base, Ohio. AD 441 216

4. Garbacz, R. J., "The Determination of Antenna Parameters by Scattering Cross-Section Measurements: II. Antenna Gain," Report 1223-9, 30 November 1962, Antenna Laboratory, The

Ohio State University Research Foundation; prepared under Contract AF 33(616)-8039, Aeronautical Systems Division, Air Force Systems Command, United States Air Force, Wright-Patterson Air Force Base, Ohio. AD 295 031

5. Garbacz, R. J., "The Determination of Antenna Parameters by Scattering Cross-Section Measurements: III. Antenna Scattering Cross Section" Report 1223-10, 30 November 1962, Antenna Laboratory, The Ohio State University Research Foundation; prepared under Contract AF 33(616)-8039, Aeronautical Systems Division, Air Force Systems Command, United States Air Force, Wright-Patterson Air Force Base, Ohio. AD 295 031

6. Handbook of Microwave Measurements (Vol. 1 and 2). Report R-352-53, PIB-286 for Signal Corps Engineering Laboratories, Contract No. DA-36-039 sc 5530. Signal Corps Project No. 26-2051-26, Department of the Army Project No. 3-27-01-122, File No. 10107-PH-51-91 (1319). Polytechnic Institute of Brooklyn Microwave Research Institute.

7. Green, R. B., "The Effect of Antenna Installations Upon the Echo Area of an Object," Report 1109-3, 29 September 1961, Antenna Laboratory, The Ohio State University Research Foundation; prepared under Contract AF 33(616)-7386, Aeronautical Systems Division, Wright-Patterson Air Force Base, Ohio. AD 274 041

8. Kennaugh, E. M., "The Echoing Area of Antennas," Report 601-14, 31 December 1957, Antenna Laboratory, The Ohio State University Research Foundation; prepared under Contract AF 33(616)-2546, Air Research and Development Command, Wright Air Development Center, Wright-Patterson Air Force Base, Ohio. AD 152 786

9. McEntee, J. A., "A Technique for Measuring the Scattering Aperture and Absorption Aperture of an Antenna," Report 612-15, 1 January 1957, Antenna Laboratory, The Ohio State University Research Foundation; prepared under Contract AF 30(635)-2811, Rome Air Development Center, Griffiss Air Force Base, New York.

10. "Radar Reflectivity Measurements Symposium," Technical Documentary Report No. RADC-TDR-64-25, Vol. II, April, 1964, Space Surveillance and Instrumentation Branch, Research and Technology Division, Air Force Systems Command, Griffiss Air Force Base, New York.